

DEVELOPMENT OF MINI ELECTROCHEMICAL MACHINING (ECM) SETUP

BY

RAJDEEP POULIK

B.Tech (Mechanical Engineering), 2021

KALYANI GOVERNMENT ENGINEERING COLLEGE, W.B.

EXAMINATION ROLL NO. - M4PRD23001

REGISTRATION NO. - 160318 of 2021-2022

THESIS

SUBMITTED IN PARTIAL FULFILLMENT OF THE REQUIREMENTS
FOR THE DEGREE OF MASTER OF PRODUCTION ENGINEERING IN
THE FACULTY OF ENGINEERING AND TECHNOLOGY

JADAVPUR UNIVERSITY

2023

DEPARTMENT OF PRODUCTION ENGINEERING

JADAVPUR UNIVERSITY

KOLKATA-700032

INDIA

JADAVPUR UNIVERSITY
FACULTY COUNCIL OF ENGINEERING AND TECHNOLOGY

CERTIFICATE OF RECOMMENDATION

THIS IS HEREBY RECOMMENDED THAT THE THESIS PREPARED UNDER OUR SUPERVISION BY **SRI RAJDEEP POULIK** ENTITLED “**DEVELOPMENT OF MINI ELECTROCHEMICAL MACHINING (ECM) SETUP**” MAY BE ACCEPTED IN PARTIAL FULFILLMENT OF THE REQUIREMENT FOR THE DEGREE OF “**MASTER OF PRODUCTION ENGINEERING**”.

THESIS ADVISORS :-

(Dr. SOUMYA SARKAR)

Professor

Dept. of Production Engineering

JADAVPUR UNIVERSITY

Kolkata – 700 032

(Dr. ASIM GOPAL BARMAN)

Associate Professor

Dept. of Production Engineering

JADAVPUR UNIVERSITY

Kolkata – 700 032

COUNTERSIGNED BY :-

HEAD

Dept. of Production Engineering

JADAVPUR UNIVERSITY

Kolkata – 700 032

DEAN

Faculty of engineering and technology

JADAVPUR UNIVERSITY

Kolkata – 700 032

JADAVPUR UNIVERSITY
FACULTY COUNCIL OF ENGINEERING AND TECHNOLOGY

CERTIFICATE OF APPROVAL*

The foregoing thesis is hereby approved as a creditable study of an engineering subject carried out and presented in a manner satisfactory to warrant its appearance as a pre-requisite to the degree for which it has been submitted. It is understood that by this approval the undersigned do not necessarily endorse or approve any statement made, opinion expressed or conclusion drawn therein but approve the thesis only for the purpose for which it is submitted.

**COMMITTEE ON FINAL EXAMINATION
FOR EVALUATION OF THE THESIS**

EXTERNAL EXAMINER

INTERNAL EXAMINER

**Only in case the recommendation is concurred in*

ACKNOWLEDGEMENT

I express my deepest gratitude to the stars that have aligned to make my post-graduation journey fruitful at Jadavpur University, a place of boundless opportunities and intellectual growth. My time at the university has been transformative, and I am indebted for the immense support and resources provided to me.

I am profoundly grateful to my esteemed thesis guide, Dr. Soumya Sarkar and Dr. Asim Gopal Barman, for their unwavering dedication, invaluable guidance, and exceptional mentorship. Their expertise, insightful feedback and continuous encouragement have been instrumental in shaping the trajectory of my research and expanding my scholarly horizons. Their passions for subject matter have been truly inspiring, and I am really privileged to have had the opportunity to work under their guidance.

I would also like to express my sincere gratitude to Dr. Bijoy Bhattacharya, the former Head of the Department, for his visionary leadership, support and academic wisdom. His commitment to fostering a vibrant learning environment has played a pivotal role in shaping my academic journey and instilling in me a deep passion for knowledge.

My heartfelt appreciation goes to the present Head of the Department, Dr. Bijan Sarkar, for his constant motivation, and steadfast belief in my potential. His guidance and commitment to academic excellence have provided a conducive environment for my research endeavors.

I extend my heartfelt thanks to the exceptional faculty members and staff of the Department for their support and expertise.

I am indebted to my incredible cohort of friends and fellow researcher scholars, especially Mr. Kingshuk Mandal and Mr. Subham Biswas, who have journeyed alongside me. Their intellectual camaraderie, stimulating discussions and support have enriched my academic experience and made it truly unforgettable.

Lastly, I would like to express my deepest gratitude to my mother Mrs. Monika Poulik, my father Mr. Uday Kumar Poulik and all my family members for their unconditional love and belief in my abilities. Thank you for the immense support. Their encouragement and sacrifices in my life have been the cornerstone of my success.

Thanking You,

RAJDEEP POULIK

CONTENTS

	PAGE NO.
TITLE SHEET	I
CERTIFICATE OF RECOMMENDATION	II
CERTIFICATE OF APPROVAL	III
ACKNOWLEDGEMENT	IV
CONTENTS	V
LIST OF FIGURES	VII
LIST OF TABLES	IX
1.0 INTRODUCTION	1
1.1 EVOLUTION OF MANUFACTURING PROCESS	1
1.2 NON-CONVENTIONAL TECHNIQUES AND THEIR NEEDS	2
1.3 SUITABILITY AND APPLICATIONS OF ECM	5
2.0 ECM - A BROAD SPECTRUM	7
2.1 INTRODUCTION	7
2.2 MATERIAL REMOVAL MECHANISM	8
2.3 THEORY AND MATHEMATICAL DERIVATION OF MATERIAL REMOVAL RATE	9
2.4 ADVANTAGES AND DISADVANTAGES OF ECM	11
2.5 PHENOMENON INFLUENCING SURFACE FINISH	12
2.5.1 SELECTIVE DISSOLUTION AND SPORADIC BREAKDOWN OF ANODIC FILM	12
2.5.2 FLOW SEPARATION AND FORMATION OF EDDIES	13
2.5.3 EVOLUTION OF HYDROGEN GAS	13
2.6 ELECTROLYTES FOR ECM PROCESS	14
2.6.1 TYPES OF ELECTROLYTES IN ECM	14
2.7 PROCESS PARAMETERS	16
2.8 ADVANCED ELECTROCHEMICAL MACHINING PROCESSES	17
2.8.1 ELECTROCHEMICAL TURNING	17
2.8.2 ELECTROCHEMICAL GRINDING	18
2.8.3 ELECTROCHEMICAL DEBURRING	19
2.8.4 ELECTROCHEMICAL MILLING	19

2.8.5 ELECTROCHEMICAL DRILLING	20
3.0 LITERATURE SURVEY	24
3.1 INTRODUCTION	24
3.2 REVIEW OF PAST LITERATURE	24
3.3 OBJECTIVES OF PRESENT RESEARCH WORK	30
3.4 SCOPES OF THE RESEARCH	30
4.0 HARDWARE COMPONENTS IN THE ECM SETUP	32
4.1 COMPONENTS USED FOR MECHANICAL SETUP	32
4.2 COMPONENTS USED FOR DEVELOPING ELECTROLYTE	
CIRCULATION SYSTEM	44
4.3 COMPONENTS USED FOR DEVELOPING MOTION CONTROL	48
4.4 COMPONENTS USED FOR DEVELOPING POWER SUPPLY SYSTEM	57
5.0 AVR C PROGRAMMING USING P-I-D CONTROL ALGORITHM	60
5.1 INTRODUCTION	60
5.2 FLOWCHART REPRESENTATION OF THE CODE	62
5.3 KEYWORDS AND THEIR EXPLANATIONS	63
5.4 VARIABLE DESCRIPTION	67
6.0 EXPERIMENTAL RESULTS AND DISCUSSIONS	68
7.0 SUMMARY AND GENERAL CONCLUSIONS	74
BIBLIOGRAPHY	77

LIST OF FIGURES

Figure no.	Title of the figure	Page no.
1.1	Schematic of basic ECM process (a) Initial stage of machining (b) Final stage of machining	6
2.1	Basic elements of ECM process	8
2.2	Schematic diagram of ECM setup	9
2.3	Schematic diagram of Electrochemical turning	18
2.4	Schematic diagram of Electrochemical grinding	18
2.5	Schematic diagram of Electrochemical deburring	19
2.6	Tool path followed by cylindrical tool in EC milling	20
2.7	Schematic diagram of Electrochemical drilling	21
2.8	ECD process of a through hole is commonly divided into four stages	22
2.9	Factors affecting the quality of hole and drilling rate	23
4.1	V-slot Aluminium extrusion	32
4.2	Corner bracket with dimensions	33
4.3	Sliding T-nut	33
4.4	CAD model of the frame	34
4.5	Schematic diagram of Bipolar stepper motor	35
4.6	NEMA 17 Stepper motor	35
4.7	Parts of a Stepper motor	36
4.8	Schematic diagram of working of Stepper motor	37
4.9	T8 Trapezoidal Lead Screw	38
4.10	Stepper motor coupled with leadscrew	39
4.11	Linear bearing and its supports	40
4.12	Corner brackets and other elements in assembly	40
4.13	Z-axis Slide	41
4.14	Linear Bearing	41
4.15	X-axis Carriage	41
4.16	Slider and Carriage in the setup	42

4.17	X-axis carriage with couplings and leadscrew in assembly	42
4.18	The assembled mechanical framework	43
4.19	Assembled framework with all parts labeled	43
4.20	Submersible pump in the setup	44
4.21	Spun filter housing	45
4.22	Booster pump in the setup	46
4.23	Assembly of electrolyte circulation system with mechanical framework	47
4.24	Arduino NANO pin description	49
4.25	Conductor developing potential difference due to Lorentz force	50
4.26	Wire through sensing unit	51
4.27	WCS 1700 Sensor Module	51
4.28	DRV8825 Sensor Module	52
4.29	Pinout diagram of DRV8825 module	53
4.30	SMPS module	58
4.31	Schematic connection diagram of the components	59
5.1	Block diagram of PID controller	60
5.2	Closed loop control strategy for tool feed mechanism	61
5.3	CTC Mode, Timing diagram	65
6.1	Hollow brass tool with insulated tip	68
6.2	Exposed hollow cross-section	69
6.3	Failures of through-hole drilling process	69
6.4	Holes drilled using P-action	70
6.5	Hole 3 drilled using P - I action	71
6.6	Holes drilled with P - I -D action	72
6.7	Circularity of holes at exit ends	73
6.8	Holes drilled with low set-point current	73

LIST OF TABLES

<u>Table no.</u>	<u>Title of the table</u>	<u>Page no.</u>
1.1	Classification of Non-conventional machining processes	3
1.2	Process capabilities of various modern machining methods	5
4.1	Logic level combinations for the step resolutions	54
5.1	TIMSK2 register map	64
5.2	TCCR2B register map	64
5.3	Clock Select Bit description	64
5.4	TCCR2A Register map	65
5.5	Variable description	67

CHAPTER 1

INTRODUCTION

1.1 EVOLUTION OF MANUFACTURING PROCESS :-

The manufacturing process, including machining, predates recorded history, dating back to around 5000-4000 B.C. During this time, tools were created to facilitate cave and rock markings and paintings. Various materials such as wood, ceramic, stone, and metals like copper, gold, iron, silver, and lead were used to produce products through casting and hammering techniques. The production of steel emerged around 600-800 A.D., prompting the development of machining methods for steel-based products. Prior to the Industrial Revolution, manual labor was the primary method of production, resulting in batch production. The Industrial Revolution originated in England in the 1750s and later spread to Europe, introducing textile machinery and advancing metal-cutting methods. The concept of using interchangeable parts emerged in the United States. Over the past century, significant advancements, including computer-integrated manufacturing, have revolutionized modern manufacturing practices.

In modern manufacturing, there are two approaches: bottom-up and top-down. The bottom-up approach, also known as additive manufacturing or 3D printing, involves creating a three-dimensional object by layering material under computer control. Examples of this approach include Stereolithography (SLA), Selective Laser Sintering (SLS), and Fused Deposition Modelling (FDM). These methods are relatively new and can produce products of various shapes and sizes using a single machine tool. However, they are limited to specific materials. Conversely, the top-down approach is referred to as subtractive manufacturing. In this approach, a three-dimensional object is produced by removing material from a solid block through cutting processes.

The top-down approach in manufacturing involves several steps, including the primary production process, material removal process, fabrication process, and finishing process.

In the primary production process, raw materials are shaped and sized to match the final product. This process encompasses casting, molding, forming, and similar techniques.

In the material removal process, excess material is removed from the primary shape of the product. Turning, milling, drilling, and similar methods are employed to achieve the desired dimensions. For larger products or those consisting of multiple parts, the fabrication process

comes into play. This involves the production of different parts that are later assembled. Fabrication processes can be permanent, such as welding, semi-permanent, such as riveting, or temporary, such as using screw-nuts and nut-bolts.

To enhance surface smoothness and meet tolerance requirements, finishing processes like grinding, lapping and honing are utilized. These processes contribute to achieving the desired surface roughness and dimensional precision of the final product.

Among the aforementioned stages of the top-down approach in the manufacturing process, the material removal process or machining process, assumes paramount significance. This machining process can be classified into two distinct categories: conventional machining and non-conventional machining. In conventional machining, a cutting tool engages in direct mechanical contact with the workpiece's surface, effecting material removal and generating chips. Turning, drilling, boring, and shaping exemplify typical instances of conventional machining processes. These processes necessitate cutting tools that exhibit superior hardness compared to the workpiece, alongside requisite traits of toughness and wear resistance.

1.2 NON-CONVENTIONAL TECHNIQUES AND THEIR NEEDS :-

Steady growing rate of demand in global scenario emphasizes the manufacturing processes to be developed to sustain the global challenges in which product can be produced within less time with greater output characteristics like better quality, precision and repeatability. Various industries, ranging from defense to medical, require more complex-shaped products made from a variety of materials, including high-strength temperature-resistant alloys, titanium alloys, stainless steel, cobalt-based alloys, fiber-reinforced composites, and ceramics. Titanium and its alloys, known for their exceptional properties such as corrosion resistance, high strength-to-weight ratio and biocompatibility, hold immense promise for diverse applications.

However, machining these materials using conventional cutting tools, poses a significant challenge in terms of effectiveness and cost-efficiency. To address this issue, non-conventional machining methods are employed. These methods, which often involve minimal or no direct contact between the tool and the workpiece (except for tool-based machining or TBM), utilize energy in its direct form to process these difficult-to-machine materials.

Non-conventional machining processes encompass four fundamental categories: mechanical, thermo-electrical, chemical, and electrochemical processes. In mechanical non-conventional processes, material removal from the workpiece is achieved by utilizing kinetic energy.

Thermo-electrical processes, on the other hand, harness energy in the form of heat to remove material by means of melting and vaporization. Chemical processes involve the use of corrosive agents to remove material from the workpiece. Lastly, electrochemical processes rely on selective ion dissolution as the mode of material removal.

Type of energy	Mechanism of material removal	Transfer medium	Energy source	Processes
Mechanical	Shear	Physical contact	Cutting tool	Tool based machining
	Erosion	High velocity particles	Hydraulic or pneumatic pressure	Abrasive jet machining (AJM), Water jet machining (WJM), Ultrasonic machining (USM)
		Ion beam	Ionised material	Ion beam machining (IBM)
Electrochemical	Ion displacement	Electrolyte	High current	Electrochemical machining (ECM)
Chemical	Ablative reaction	Reactive environment	Corrosive agent	Chemical machining (CHM)
Thermoelectric	Fusion	Hot gases	Ionised material	Plasma arc machining (PAM)
		Electrons	High voltage	Electron beam machining (EBM), Electro-discharge machining (EDM)
	Ablation	Radiation	Amplified light	Laser beam machining (LBM)

Table 1.1: Classification of Non-conventional machining processes

Mechanical Processes such as Abrasive Jet Machining (AJM), Ultrasonic Machining (USM), and Water Jet Machining (WJM) utilize the kinetic energy of abrasives or water jets to carry out the metal removal process. However, the effectiveness of these mechanical processes is limited by the dependency of hardness, strength, and other physical and mechanical properties on their performance index. This limitation has led to the emergence of modern thermo-electrical machining processes.

Thermo-electrical processes involve the removal of material through the application of supplied energy in various forms, such as electric discharge (EDM), electron beam (EBM), heat (PAM), or light (LBM). EDM, for instance, finds extensive use in machining hard and tough electrically conductive materials, but it may have limitations when higher surface finish, higher material removal rate (MRR), and minimal damage to the work surface are the primary requirements.

Hybrid machining processes combine two or more different machining methods to enhance the overall efficiency of the machining process. Electro Discharge Grinding (EDG), Electrochemical Grinding (ECG), and Electrochemical Discharge Machining (ECDG) are examples of hybrid processes that have been developed to leverage the advantages of their constituent processes.

Efficient utilization of modern machining processes requires a comprehensive understanding of their nature and capabilities. While these methods do not completely replace conventional machining techniques, they are crucial in specific situations. Therefore, it is important to assess the suitability of these methods based on the given conditions. Table 1.2 portrays the process capabilities of different modern machining methods. Making an appropriate selection of these methods for a specific machining task is essential.

Process	MRR (mm ³ /min)	Tolerance (μm)	Surface (μm) CLA _e	Depth of surface damage (μm)	Power (Watts)
USM	300	7.5	0.2-0.5	25	2400
AJM	0.8	50	0.5-1.2	2.5	250
ECM	15000	50	0.1-2.5	5.0	100000
CHM	15	50	0.5-2.5	50	--
EDM	800	15	0.2-1.2	125	2700
EBM	1.6	25	0.5-2.5	250	150
LBM	0.1	25	0.5-1.2	125	2 (average)
PAM	75000	125	Rough	500	50000
Conventional	50000	50	0.5-5.0	25	3000

Table 1.2: Process capabilities of various modern machining methods

1.3 SUITABILITY AND APPLICATIONS OF ECM :-

While EDM and LBM are thermal processes that can result in heat-affected zones and micro-cracks, ECM avoids such issues by eliminating thermal and mechanical stresses on the workpiece. ECM offers versatility in machining various materials. It provides higher material removal rates, improved precision by controlled material removal. ECM has found applications in aerospace, defense, medical, automobile and turbo-machinery industries due to its advantages, thereby making it a promising technique for complex shape machining of high-strength and thermal-resistant materials.

Electro-chemical machining relies on the principles outlined in Faraday's laws of electrolysis. The work-piece connects to the positive terminal, gets designated as anode, while the tool connects to the negative terminal, gets designated as cathode. Both are immersed in an electrolyte solution, which serves as the conductive medium and completes the circuit. By applying a sufficient potential difference between the cathode and the anode, a

current is induced, and ionic dissolution occurs. Material removal takes place atom by atom through this process.

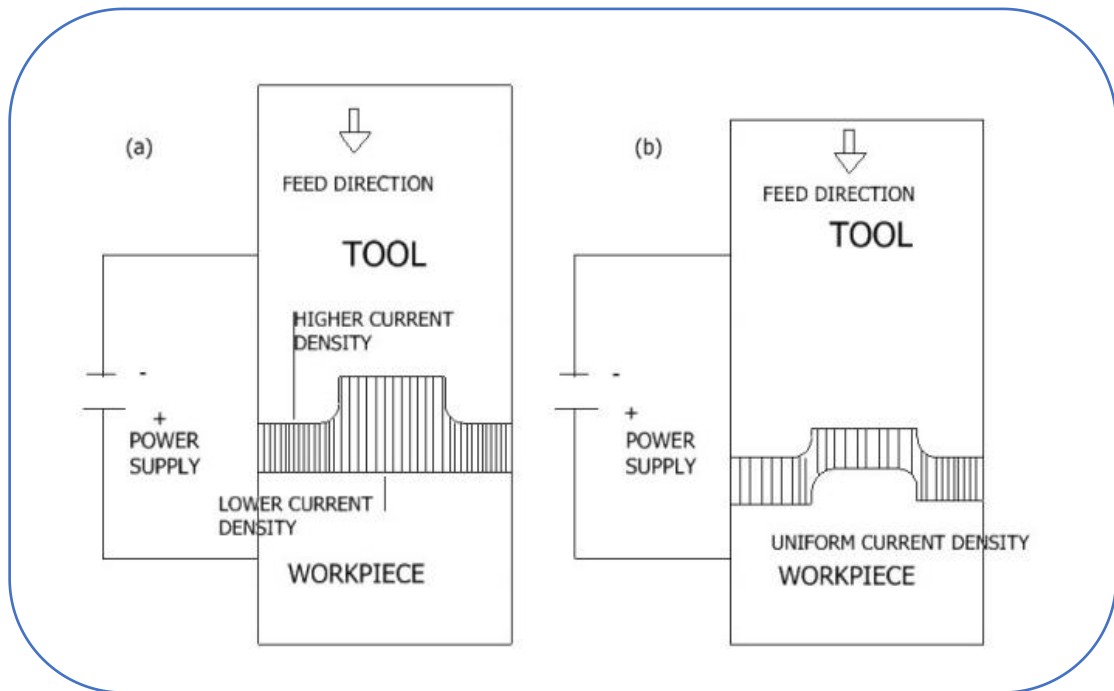


Figure 1.1: Schematic of basic ECM process

(a) Initial stage of machining (b) Final stage of machining

Fig. 1.1 shows the schematic diagram of the ECM process. As shown in Fig. 1.1(a), at the first stages of machining, the current density is relatively higher at the zone where the gap between tool and the workpiece is less because of the geometry of the tool. Fig. 1.1(b) shows the last stages of the machining when the gap between tool and the workpiece is same everywhere resulting in same current density.

2.1 INTRODUCTION :-

Electrochemical machining (ECM) has gained significant recognition as a non-traditional manufacturing process in the industry. It involves the controlled removal of metal through anodic dissolution in an electrolytic medium, with the workpiece serving as the anode and the tool as the cathode. Unlike other machining processes, ECM operates without any physical contact between the tool and the workpiece. Instead, metal is dissolved atom by atom, providing a gentle and precise method of material removal.

While ECM appears conceptually simple, its reliance on electrical, chemical and electrolyte flow phenomena presents challenges for a comprehensive understanding. Processes such as electroplating and electropolishing, rooted in Faraday's work, have already been well-established in manufacturing industries. The use of chemical phenomena for material removal traces back to 2500 B.C., when Egyptian artisans etched copper jewelry using citric acid. However, it wasn't until 1959 that Anocut Engineering Company of Chicago introduced the concept of anodic metal removal as commercial equipment for regular industrial applications.

ECM exhibits immense potential due to its versatility and wide range of applications, positioning it as a promising, successful, and commercially viable machining process. The concept of anodic metal removal as a metalworking technique was initially suggested by W. Gusseff and later expanded upon by C.F. Burgess in 1941. Gusseff obtained the first patent for ECM as early as 1929, proposing a method that combined chemical and mechanical means for machining. In 1940, Gusseff developed the foundation for the ECM processes known today. ECM was first introduced in the aerospace and aircraft industries during the late fifties and early sixties, primarily for shaping, deburring, and finishing operations on large parts. However, achieving high accuracy and fine surface finishes in ECM poses challenges in selecting the appropriate working parameters. The determination of suitable ECM parameters becomes crucial for attaining the desired level of precision and surface quality. Basic elements of ECM process are presented in figure 2.1.

ECM is particularly well-suited for machining hard and high-alloyed materials, which find extensive use in aerospace and biomedical engineering applications. One notable advantage of ECM is its ability to effectively handle complex shapes, including curvilinear shapes and

contours. The wide-ranging applications and effectiveness of ECM in cutting hard materials with intricate geometries make it a crucial process in modern manufacturing. To further enhance the utilization of ECM, it is imperative to conduct thorough investigations into the characteristics of the machined surface. This entails comprehensive research, including parametric analysis, to examine the impact of various factors on the surface parameters of the machined component during ECM. Such endeavors will contribute to the successful implementation and advancement of ECM in contemporary manufacturing practices.

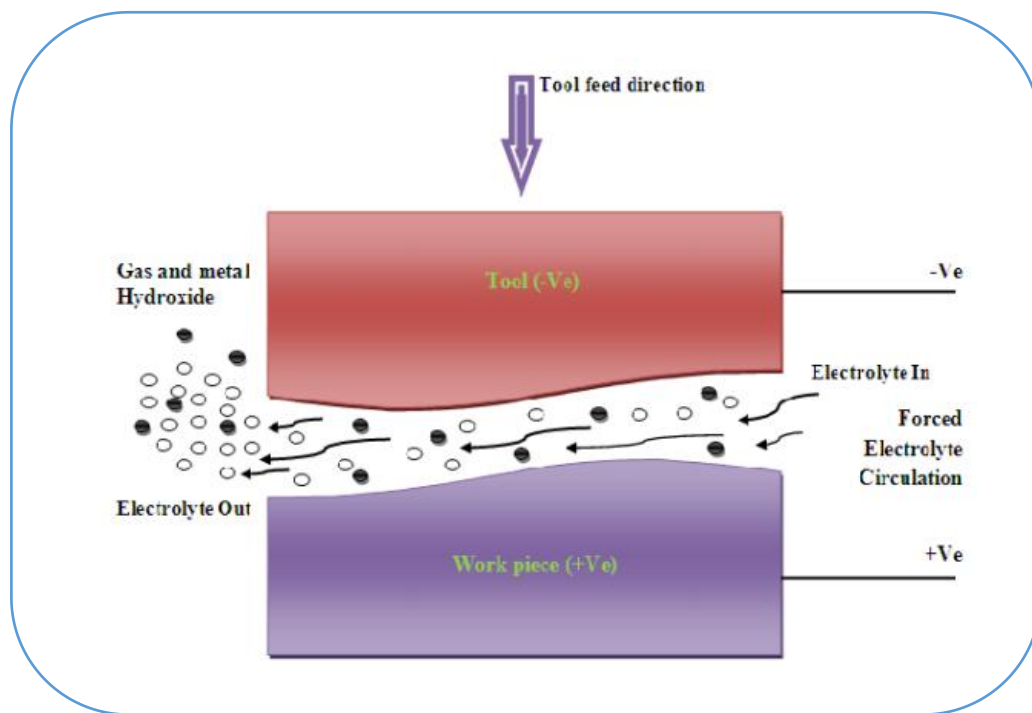


Figure 2.1: Basic elements of ECM process

2.2 METAL REMOVAL MECHANISM :-

The fundamental principle behind electrochemical machining (ECM) lies in the process of electrolysis. Electrolysis is a chemical reaction that occurs when an electric current passes through a liquid solution, with two conductors immersed in it. The presence of an electric circuit can be confirmed by using an ammeter, which indicates the flow of current. The liquid solution used in ECM acts as an electrolyte, enabling the conduction of electricity and completing the circuit. Figure 2.2 shows the schematic diagram of ECM setup.

During electrolysis, chemical reactions take place at either the anode or the cathode, resulting in anodic or cathodic reactions, respectively. The key distinction between metallic

conductors and electrolytes is that in metals, current is carried by electrons, whereas in electrolytes, it is carried by ions. Ions are atoms that have gained or lost electrons, acquiring a positive or negative charge. Positively charged ions migrate toward the cathode, while negatively charged ions move toward the anode. To maintain neutrality within the electrolyte, there must be a balance between the total positive and negative charges. Consequently, one electrode loses material while the other gains an equal amount, allowing for both material removal and addition. Electrolysis finds significant applications in electroplating and electro-polishing processes.

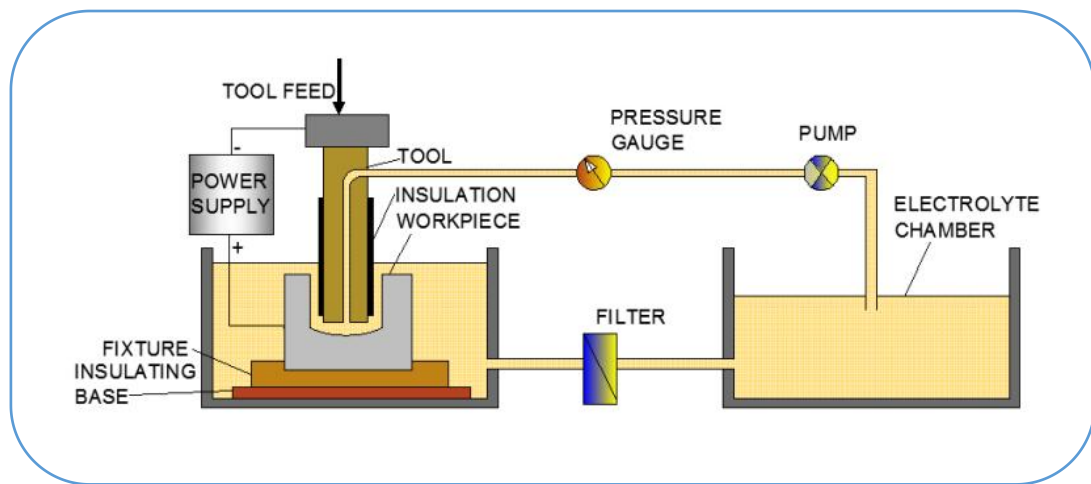


Figure 2.2: Schematic diagram of ECM setup

2.3 THEORY AND MATHEMATICAL DERIVATION OF MATERIAL REMOVAL RATE :-

The amount of material removed is determined by Faraday's first law which states that the mass of the substance removed at an electrode is proportional to the quantity of current passed to that electrode. So,

$$V = C * I * t$$

where,

V = volume of metal removed (mm³)

C = electrochemical constant (mm³ /amp-s)

I = current (amps)

t = time (sec)

The electrochemical constant is unique for every work material and the above equation can be written as,

$$C = \frac{M}{Z * F}$$

where,

M = molecular mass

Z = number of valence electrons

F = Faraday's constant

According to Ohm's law, current **I** can be related as,

$$I = \frac{E}{R}$$

where,

E = voltage

R = resistance

The resistance **R** for ECM operations is given as,

$$R = \frac{g * r}{A}$$

where,

g = gap between the tool and the workpiece (mm)

r = resistivity of the electrolyte (ohm-mm)

A = surface area of tool (mm²)

Hence, **MRR** (in mm³/s) is given as,

$$MRR = \frac{V}{t} = \frac{C * E * A}{g * r}$$

These equations were derived assuming 100% efficiency.

2.4 ADVANTAGES AND DISADVANTAGES OF ECM :-

Electro-chemical machining offers several advantages over other competing technologies. These advantages have made ECM the best choice for a variety of applications. The advantages are as follows:

- (i) The product is free of burrs after processing.
- (ii) This is a non-contact process, hence
 - The process does not cause thermal or physical strain on the product.
 - Unlike other machining techniques, no upper-layer deformation occurs.
- (iii) 3-Dimensional products can be processed in one single step.
- (iv) High quality surface finish level attainable ($R_a < 0.05 \mu\text{m}$) depending on material.
- (v) Products of complex shapes with high dimensional accuracy are attainable.
- (vi) Material stress which releases during the process will be compensated where possible.
- (vii) Stainless steel in the upper-layer will be affected through various machining techniques, as a result of which local rust formation can occur. This is not the case with ECM.
- (viii) Independence from Material Properties: The machining or dissolution rate in ECM is not influenced by the hardness or other mechanical and physical properties of the material. For the machining of the product it is also irrelevant if it is processed before or after a heat treatment (hardening) step.
- (ix) Material removal rate is high, approximately $1.5 \text{ cm}^3/\text{min}$ by 1000A direct current..
- (x) Versatile Machining Capability: ECM can efficiently machine hard and brittle materials that are electrically conductive, including challenging-to-cut materials like Ti-based alloys and Ni-based alloys.
- (xi) Initial investments in process design and electrode construction are high, however the recurring costs are low.
- (xii) Tool Longevity: Only hydrogen gas is evolved at the cathode, and the tool remains unchanged. This means that the same tool can be used for subsequent ECM operations. Soft conductive materials like copper or brass can be used as ECM tools.

(xiii) **Minimal Tool Wear:** Since there is no direct contact between the tool and the workpiece in ECM, there is no tool wear. This eliminates issues associated with mechanical force application, such as crack propagation and in-homogeneous stress distribution.

Although ECM offers significant advantages for precise and efficient machining of conductive materials, ongoing research is being conducted to explore various aspects of the process.

The disadvantages are as follows:

- (i) ECM was previously known as an environmental unfriendly process. Through developments in the treatment of electrolytes, the process has become less harmful to the environment. The sludge can be re-used depending on the machined material.
- (ii) Each product and material requires new research.
- (iii) Higher production numbers are essential, as a special electrode must be developed for each product. The ultimate best depends on complexity and material.
- (iv) High power consumption but in general lower than other non-conventional machining techniques.
- (v) Design of electrode is complex and initially expensive.
- (vi) ECM requires relatively high skilled staff.

2.5 PHENOMENON INFLUENCING SURFACE FINISH :-

Generally very good surface finish is desired in the parts machined by ECM, a study of the possibilities that may result in a bad finish is important. The surface finish is adversely affected by the (i) selective dissolution and sporadic breakdown of anodic film (ii) flow separation and formation of eddies, and (iii) evolution of hydrogen gas.

2.5.1 SELECTIVE DISSOLUTION AND SPORADIC BREAKDOWN OF ANODIC FILM :

Surface finish produced by electrochemical machining process using various materials and electrolyte combination depends basically on the electrochemical phenomenon between the two. The variation of etching characteristics of different phases of alloy crystalline structure determines the surface texture, and sporadic breakdown of the anodic film permitting

intermittent machining at localized sites is the controlling factor in deciding the surface finish. In both phenomenons, increased potential gradient across the electrolyte film improves surface finish. Due to different metallurgical structures there are individual sites available on the surface of the work piece, which possesses different etching properties on the surface. Because of this aspect, the anode surface, which is exposed to the approaching cathode, will vary in their distances from the cathode surface. Thus individual grain that readily etches will be recessed into the anode surface. Hence fine grain structure will tend to produce a smooth surface and vice versa. A single phase material with single crystal components will produce the best finishes.

Generation of surface texture also depends on potential gradient close to the anode surface. Higher the potential gradient better will be the finishing, since poor etching phase of material has to be less exposed to potential to maintain overall dissolution rate. The current density is one of the process variables that can control potential gradient substantially within the anode layer. Hence improvement in surface finish can be achieved by increasing the current density.

2.5.2 FLOW SEPARATION AND FORMATION OF EDDIES :

The presence of hills and valleys on the anode surface may cause a separation of electrolyte flow and eddy formation. In these eddies, separated from the main stream, a large concentration of the metal ions may build up, resulting in a high concentration over potential in the eddies. This introduces a localized variation in the removal rates, and consequently an uneven finished surface. Apart from the presence of hills and valleys, the flow separation may be caused by an improper design of the tool and the electrolyte flow path. So, a great care has to be taken in designing the electrolyte flow path in a tool.

2.5.3 EVOLUTION OF HYDROGEN GAS :

The flowing electrolyte collects the evolving H_2 gas generated at the cathode. The presence of H_2 in the electrolyte reduces the specific conductivity of the solution. This effect increases as the H_2 concentration goes on increasing downstream, and the overall effect is a deterioration of the surface finish.

2.6 ELECTROLYTES FOR ECM PROCESS :-

In electrochemical machining, the electrolytes play an important role. Electrolytes are used for electrochemical machining have many functions to perform during the actual machining process. Some of the important functions performed by the electrolyte are listed below:

- (i) It completes the electrical circuit between the tool and work piece.
- (ii) It causes the metal removal through chemical and electrochemical reactions.
- (iii) It carries away the heat which is generated in the machining zone due to flow of high current through it.
- (iv) It removes the by-products of electrolysis from the small machining gap.

Hence, an electrolyte is to be chosen for ECM which should possess some or all of following desirable characteristics for successful operation of ECM practice:

- (i) It should be of high electrical conductivity.
- (ii) Its viscosity should be low and should be of higher specific heat.
- (iii) It should provide chemical stability and resistance to formation of passivating film on work surface.
- (iv) Machining can be done with electrolyte having higher current efficiency.
- (v) It should be non-corrosive to the equipment, fixtures, tooling and work material.
- (vi) It should be non-toxic and safe in its use.
- (vii) It should be inexpensive and readily available etc.

2.6.1 TYPES OF ELECTROLYTES IN ECM :

The electrolytes used for ECM may be classified into following two types:

- (i) Electrolytes which produce insoluble reaction products or sludge immediately after the passage of machining current e.g. while using NaCl salt solution being known as Neutral type electrolyte, sludge and precipitates of the dissolved metal are produced.
- (ii) Electrolytes which cause the production of soluble sludges i.e. no electrochemical precipitates are found e.g. strong acids like HCl, H₂SO₄ electrolytes or strong caustic solution cause to produce soluble sludge.

For the first type, the composition of the electrolyte may be kept unchanged by maintaining volume of electrolyte constant with the addition of distilled water so as to maintain pH value. But these electrolytes have got some disadvantages:

- (a) They cannot machine some metals such as tungsten, titanium etc.
- (b) Poor surface finishes may be produced on silicon based bearing alloys.
- (c) Large volumes of sludge are produced during machining which must be removed from the machining zone to some established level.
- (d) They are moderately corrosive in nature. Viscosity of electrolytes increases with sludge formation. This becomes of particular importance in case of machining with high electrolyte flow velocities and small gaps where a low viscosity of electrolyte is desirable. Moreover, the sludge removal requires high filtration capacity.

However, in case of the second type of electrolytes, the most predominant phenomenon compared with first type electrolyte has been change of composition of the electrolyte which is difficult to control. Moreover, the various demerits of such type of electrolytes are important for consideration. The various disadvantages of acidic type electrolytes are as follows:

- (i) They are corrosive to machine parts, may attack the workpiece chemically and cause the surface finish to be poor.
- (ii) The workpiece ions have got more possibility of being soluble and have greater tendency to plate out on to the cathode or tool, which can be prevented by using high flow rates.

The disadvantages of the alkaline type of electrolytes are cited below:

- (i) These tend to form passivating films on the work piece surface of most metals causing the machine to be either impossible or non-uniform.
- (ii) Alkaline solutions are dangerous so they require careful handling.
- (iii) These may also attack some machine parts and cause damage of the parts.

All these important facts must be considered before choosing the best electrolyte for the specific purpose of ECM operation.

NaCl in water has found to be suitable for most of the applications but corrosiveness is major problem like other electrolyte. Since sodium nitrate is less corrosive and possess other desirable properties, it is extensively used electrolyte for ECM process. However its lower conductivity and tendency to passivate chemical reaction makes it unsuitable for adoption to all ECM applications.

Other alkaline chemicals employed for this purpose are potassium nitrate, sodium sulphate, sodium chromate, sodium hydroxide, sodium fluoride, potassium chloride and sometimes a mixture of two or more of these chemicals are best suited for an efficient electrolyte. Ti₆Al₄V is considered as good corrosion resistance material due to existence of passive oxide film, however due to this, it shows great difficulty in carrying out electrochemical machining of this material. With simple chloride and nitrate electrolyte, high voltage is required to achieve machining through this passive film. It has been reported that voltage required to break down the passive film can be reduced by the use bromide and iodide electrolyte.

2.7 PROCESS PARAMETERS :-

The conventional machining processes are self controlling in nature due to the fact that a steady state metal removal is available when tool feed rate and other controlling parameters are steady. But in ECM, the various physical, chemical and hydrodynamic phenomena occur in the machining gap during the course of operation. The machining rate at any instant depends not only on the end gap but also upon other process parameters such as electrolyte flow rate, applied voltage, concentration of electrolyte and tool feed rate.

The rate of metal (anodic) dissolution is proportional to the amount of current/ current density in inter-electrode gap thickness. This machining current more or less depends on electrolyte concentration, inter-electrode gap thickness, applied voltage and tool feed rate. Hence it is desirable to study effects of following parameters as mentioned below for analysis of material removal rate during the ECM. The type of finish obtained in an ECM operation is dependent on the material, electrolyte and current density. If the surface finish obtained is not upto the required standard, then some adjustment in machining parameters is needed to be done. Electrolyte composition is the prime factor in the anode potential characteristics of the electrochemically machined surface. Selection of electrolyte is, therefore, a most effective way of obtaining surface finish improvement.

The accuracy of the work piece dissolution as well as ECM process stability for post machined surface profile is decided by setting, maintaining and controlling the process parameters during the process. However, in order to achieve the effective and high precision machining, the following major process parameters of the ECM system will have to be optimally controlled:

- (i) Applied voltage,
- (ii) Machining current,
- (iii) Electrolyte and its concentration,.
- (iv) Electrolyte flow type and flow velocity,
- (v) IEG i.e. gap between the tool and work piece, and
- (vi) Tool feed rate, etc.

2.8 VARIOUS ADVANCED ELECTROCHEMICAL MACHINING PROCESSES :-

Electrochemical machining process has been used in several machining field for its excellent utility. Electrochemical machining process either can directly act to remove material in different machining technique or it can assist other machining processes to remove material. Several advanced ECM processes are as follows:

2.8.1 ELECTROCHEMICAL TURNING :

In case of electrochemical turning (EC Turning), electrochemical machining technique has been employed for turning operation. In EC turning, workpiece is rotated and connected with positive terminal. Tool is attached with tool feed motion and connected with negative terminal. Both the tool and job are submerged in electrolyte solution. When a potential difference is applied across the tool job interface, material is removed from the job. As the job is rotated, homogeneous dissolution is occurring from all sides of the job. It has been shown on the Fig. 1.2, the schematic diagram of the working principle of the EC turning process. By controlling the motion of the tool, thickness of the workpiece is obtained. Job is insulated except the machining zone to restrict the material removal from required portion.

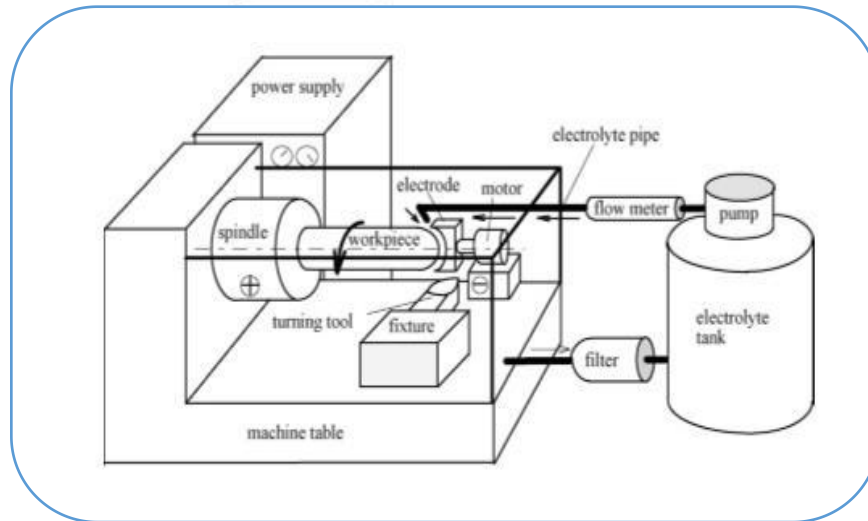


Figure 2.3: Schematic diagram of Electrochemical turning

2.8.2 ELECTROCHEMICAL GRINDING :

In case of electrochemical grinding (ECG), grinding operation is carried out with the help of electrochemical machining principle. In this type of operation, negative potential is given to the grinding wheel whereas positive potential is given to workpiece. High velocity electrolyte jet is supplied in between job and wheel. Grind wheel with metallic bond is rotated with high velocity and the workpiece moves along X direction parallel with the wheel. Thus surface finishing is occurred as material is removed from the uneven surface of the job and it is possible to attain great surface quality. In the figure 2.4, the schematic diagram of the working principle of the ECG has been shown.

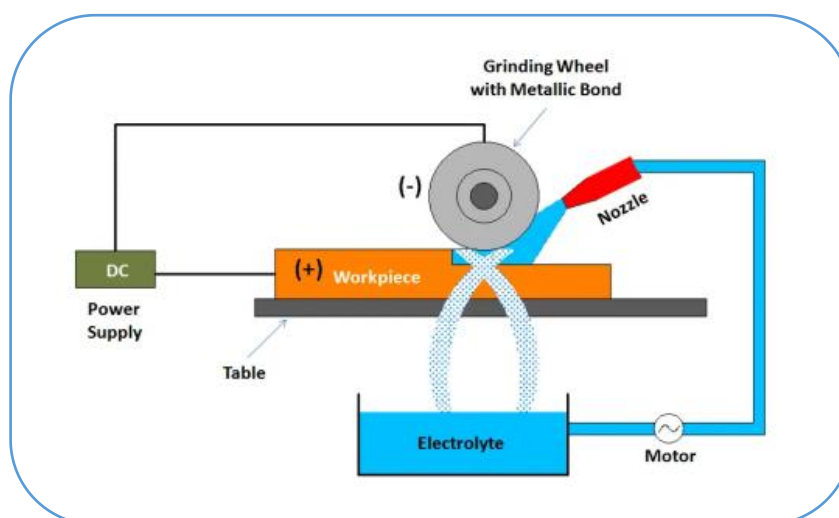


Figure 2.4: Schematic diagram of Electrochemical grinding

2.8.3 ELECTROCHEMICAL DEBURRING :

Electrochemical deburring (ECD) is an advanced application of electrochemical principle where burrs are removed from the job [4]. In the figure 2.5, the schematic diagram of working principle of ECD has been shown. A tool connected with negative terminal of a DC power source acts as cathode and job is connected with positive terminal. To restrict the material removal from the job other than burrs either the tool or the job is insulated depending on the condition. Electrolyte flow is given into the tool job channel and the burr is removed from the job by the dissolution into the solution.

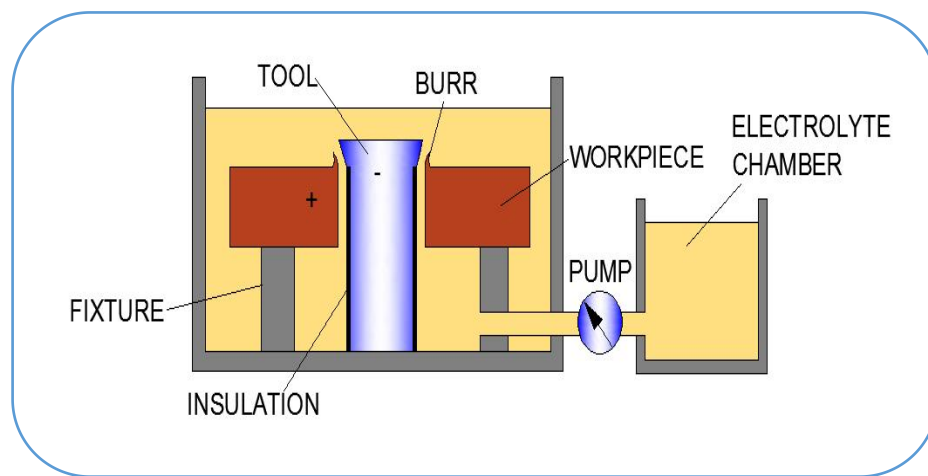


Figure 2.5: Schematic diagram of Electrochemical deburring

2.8.4 ELECTROCHEMICAL MILLING :

In case of Electrochemical milling (EC milling) the material removal mechanism is as same as in conventional ECM where electrochemical dissolution occurs from anode (workpiece) when voltage difference is applied across tool (cathode) and workpiece (anode). The tool shape complexity of the ECM process can be resolved in the EC milling process where a simple geometrical shape tool used as cathode. In this process the job is connected to the positive terminal and the tool is connected to the negative terminal of a pulse or constant DC power source. This process is used for generation of complex feature. As like conventional end milling, tool moves along a predetermined path in case of EC milling. With the help of a simple geometrical tool material can be removed in layer by layer fashion. In the figure 2.6,

‘S’ is the machining starting position and ‘P’ is the present position of the tool while machining is going on. The tool moves along the predefined path in a layer-by-layer fashion to achieve a desired geometry over the workpiece as shown in the figure. After the removal of material from one layer, the process is further repeated until the final desired depth is obtained and this layer is termed as milling layer thickness. Thus, the way of generating final desired profile of this process resembles with conventional end milling process. Different profiles can be machined through controlling the relative movement between tool and the job along with X, Y and Z axis.

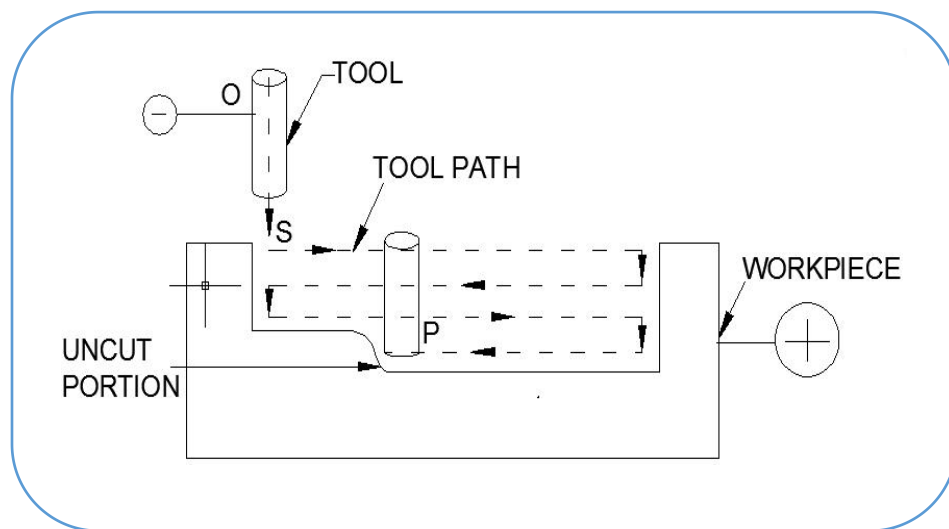


Figure 2.6: Tool path followed by cylindrical tool in EC milling

2.8.5 ELECTROCHEMICAL DRILLING :

Electrochemical drilling (ECD) is an unconventional drilling process that removes material, which is generally metal, from the workpiece by controlled electrochemical dissolution accordingly to Faraday's law. Electrochemical drilling utilizes a side-insulated hollow tube as the cathode tool and removes anodic material in an electrolytic cell. It inherits various merits from electrochemical machining, including independence from the material mechanical properties, an absence of tool wear and residual stresses, and good surface integrity. Thus, ECD has attracted much attention as an alternative method for producing small holes. When a voltage difference is applied, the anodic material is electrochemically dissolved and a hole is

gradually generated by continuously feeding the tube electrode, as schematically illustrated in figure 2.7

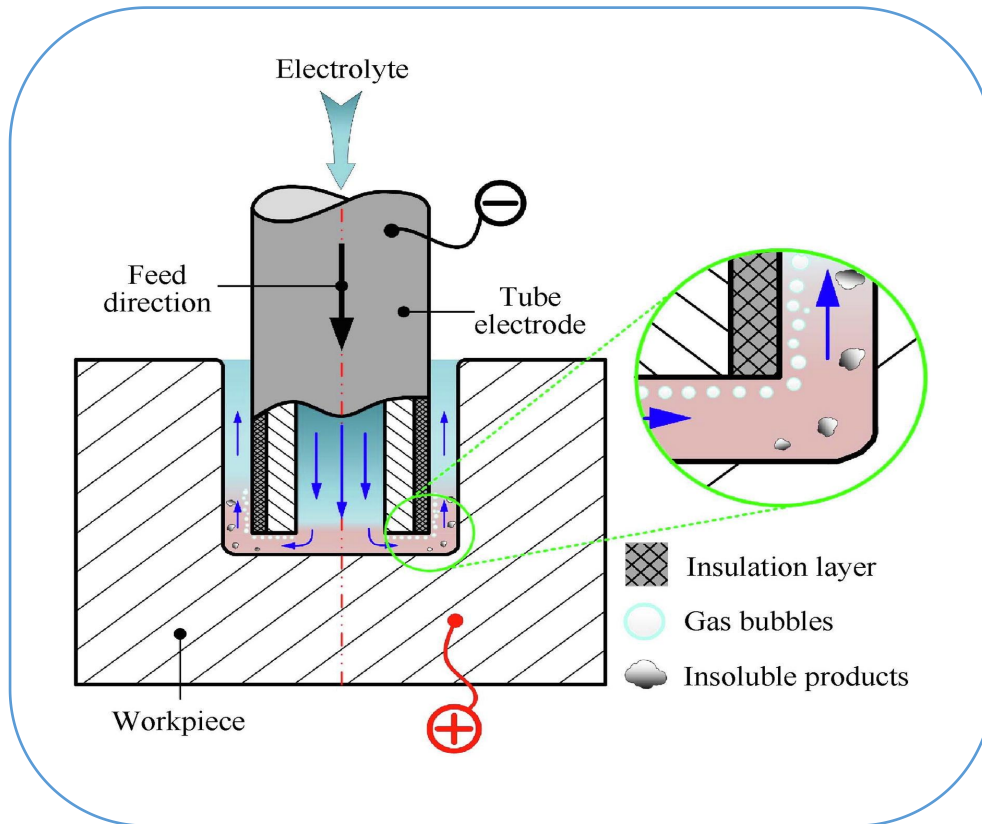


Figure 2.7: Schematic diagram of Electrochemical drilling

In industry, acid electrolyte solutions are employed for drilling holes with small tolerances and high aspect ratio, as they avoid the production of insoluble precipitates and improve the process stability. However, acid electrolytes are unfriendly to the environment and their waste disposal is expensive. Thus, neutral salt solutions have been increasingly adopted in ECD. The type of solution generally favoured for electrolytes are sodium chloride, sodium nitrate, sodium chlorate or a combination of these. When a neutral salt electrolyte is used, the dissolved metallic ions usually react with hydroxyl ions to form insoluble waste products, which may accumulate progressively and block the machining gap. This can exert a negative impact on the process stability and the machining accuracy. Therefore, some methods are used to sweep machining products away rapidly in electrolyte flow pattern. Using a pulsed current can enhance the removal of electrolysis products during the pulse-off time and lead to stable machining. The electrolyte flux directly determines the electrolyte flow velocity at the

machining gap, which removes machining products and accelerates the renewal of electrolyte in the gap. The electrolyte also prevents heat from building up in the machining area.

There are many advantages for electrochemical drilling that makes it unique and they are

- (i) drilling rates can easily be controlled by electric current,
- (ii) type of electrolytes that do not harm environment
- (iii) absence of heat affected zones and mechanical stresses
- (iv) does not alter work piece properties
- (v) stainless steel or titanium can be drilled
- (vi) able to drill multiple holes at one instance.

The tool chosen for drilling should have the following characteristics:

- (i) excellent mechanical and electrical properties
- (ii) adequate stiffness to overcome electrolyte compression
- (iii) able to withstand corrosive solutions
- (iv) conductor of heat and poses excellent machinability.

The choice of tool should be appropriate for the material properties of the workpiece.

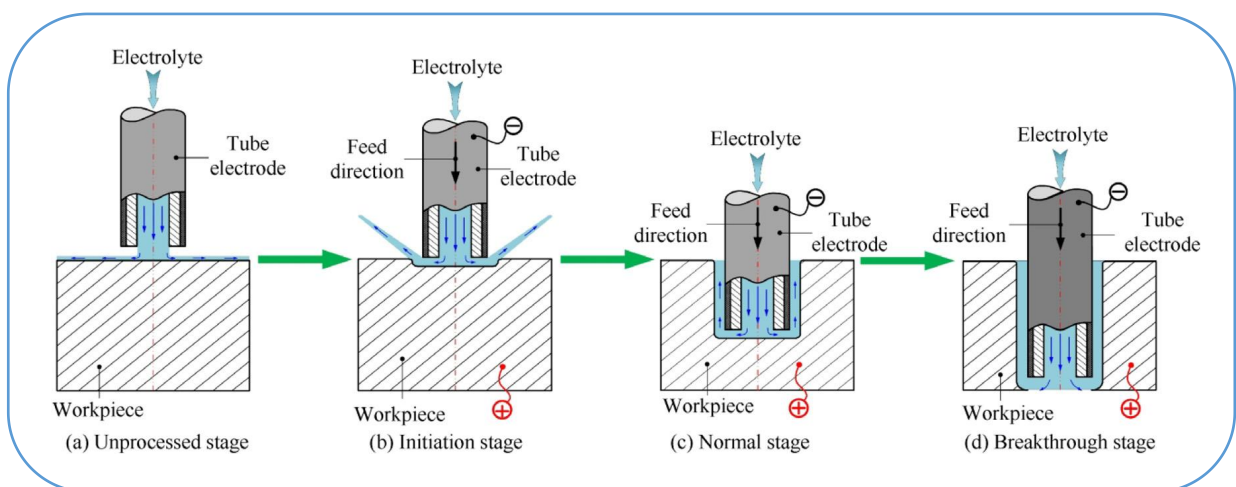


Figure 2.8: ECD process of a through hole is commonly divided into four stages.

Hole quality and surface roughness are generally influenced by factors like pulse current, frequency, inter-electrode gap, type and tool shape, flow rate of electrolyte and of course the concentration of electrolyte. Common types of circular hole features achieved from electrochemical drilling are overcut, aspect ratio and hole taper. Overcut is defined as half the size after deducting hole diameter from tool diameter. Taper angle can be measured using hole entrance diameter and the size of the exit of holes. One of the greatest issues faced in ECD is the formation of taper. Taper angle for blind hole is normally greater than through hole. This is firstly, it is not easy for the electrolyte to penetrate deep into hole as is difficult to dissolve the metal. The second reason is due to boiling of electrolyte; bubbles are formed that are stuck in small machining opening which raises the resistance against dissolve of subtract. This will then cause the current to flow from the side to entrance of the hole which will cause the hole to be enlarged. The third reason is due to chemical reaction to dissolve subtract. As during that process, chromium oxide layer is developed which will then stop the dissolution process. Lastly, taper is created because of the gap in between the drilling time in the middle of both top and bottom hole, as taper reduces as tool feeds through the holes.

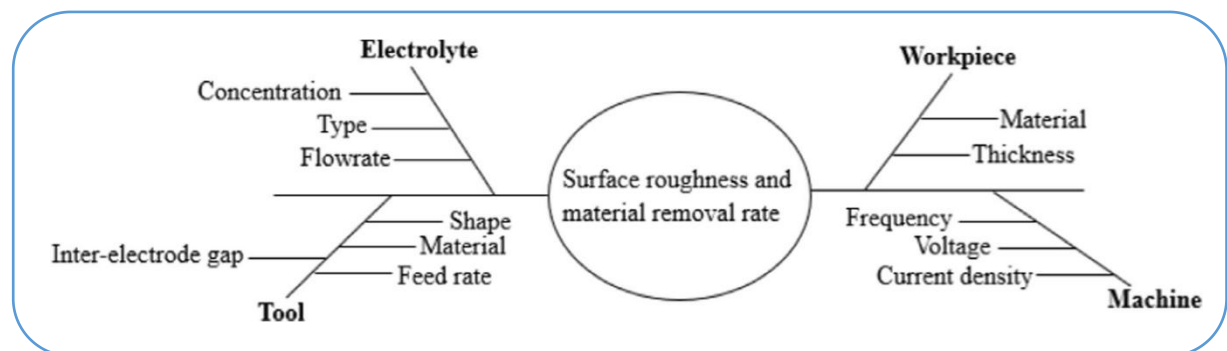


Figure 2.9: Factors affecting the quality of hole and drilling rate

3.1 INTRODUCTION :-

Michael Faraday had established the laws of electrolysis in the beginning of 19th century. These laws are fundamentals behind the principle of electrochemical dissolution. In 1929 researcher W. Gusseff first developed the process to machine material through electrolytic process. Since the time, ECM had been developed and still advancement of the process is going on. ECM has received industrial importance due to its various advantages. ECM also has various challenges those have been addressed by researcher to make the process more effective. Researchers are trying very hard to overcome these problems and investigations from different research work have been documented in this section.

3.2 REVIEW OF PAST LITERATURE :-

Dayanand S. Bilgi et al. [1] presented an experimental investigation on pulse-current shaped-tube electrochemical deep hole drilling (PC-STED) of nickel-based super-alloy. The study focused on examining the influence of five process variables, namely voltage, tool feed rate, pulse on-time, duty cycle, and bare tip length of the tool, on three key responses: depth-averaged radial overcut (DAROC), mass metal removal rate (MRRg), and linear metal removal rate (MRRl). Mathematical models had been developed to capture the effects of the process parameters on DAROC, MRRg, and MRRl. These models enable a quantitative evaluation of hole quality and process performance simultaneously. The experimental results confirmed the validity of the models in predicting the profile of the drilled hole and MRRl. Throughout the experiments, through holes of 26 mm depth and diameters ranging from 2.205 mm to 3.279 mm were successfully drilled. The findings can be attributed to the dynamics of the inter-electrode gap during pulse electrochemical deep hole drilling. The optimized parameters identified from these experiments can be employed to efficiently drill high-quality, high aspect ratio deep holes in nickel-based super-alloys.

B. Bhattacharyya et al. [2] focused on investigating the influence of various electrochemical micromachining parameters, including machining voltage, electrolyte concentration, pulse period, and frequency, on material removal rate, accuracy, and surface finish at the

microscopic level. The experimental study reveals that optimal values for micro machining parameters are 3 V for machining voltage, 55 Hz for frequency, and 20 g/l for electrolyte concentration, resulting in enhanced accuracy and maximum material removal. SEM micrographs demonstrate that low voltage, moderate electrolyte concentration, and high frequency contribute to improved accuracy with fewer micro-sparks. The research also considers factors such as radial stray cut and on-line pulse pattern to identify the most effective zone of EMM parameters. The findings of this research present new opportunities for the effective utilization of electro-chemical material removal mechanisms in the field of micro-manufacturing.

Alexandre SPIESER et al. [3] focused their research on the design of a next-generation μ ECM machine catering to the automotive, aerospace, medical, and metrology sectors. The machine incorporates three axes of motion (X, Y, Z) and a spindle that enables the tool-electrode to rotate during the machining process. To ensure ultra-precise motion, the machine employs linear slides with air bearings, linear DC brushless motors, and 2 nm-resolution encoders. The control system relied on the Power PMAC motion controller from Delta Tau. The electrolyte tank, situated at the rear of the machine, allowed for quick electrolyte changes. Notably, the machine featured two process control algorithms: fuzzy logic control and adaptive feed rate. Furthermore, a self-developed pulse generator had been integrated into the machine and connected to a wire ECM grinding device. The pulse generator offered the flexibility to reverse the pulse polarity for on-line tool fabrication.

A. W. Labib et al. [4] developed a fuzzy logic controller to enhance the ECM process. The existing control system of an experimental ECM drilling rig at the University of Manchester was upgraded by integrating a fuzzy logic controller. Matlab, specifically the Fuzzy Logic Toolbox, was utilized to construct the fuzzy logic controller system responsible for regulating the tool's feed rate and the electrolyte's flow rate. The primary goal of the fuzzy logic controller was to optimize machining performance and accuracy by effectively controlling the ECM process variables. The outcomes of this study showcased the innovative possibilities and potential applications of fuzzy logic control (FLC) in ECM, allowing for intelligent decision-making akin to human-like intelligence. While this paper focused on the feasibility of FLC in ECM, the results held promise for Electro-chemical micro machining (EMM) as well. As ECM progresses towards EMM, the implementation of FLC as a means of process uncertainty control offers distinct advantages over conventional control methods.

Chaojiang Li et al. [5] developed a novel approach combining high-speed self-adjusting electrical discharge machining (EDM) and electrochemical machining (ECM) to enhance the surface quality of film cooling holes and minimize the thickness of the recast layer, . This approach incorporated two independent flushing systems that could automatically switch during the machining process. The flushing systems utilized different work-liquids and dynamically adjusted discharge parameters online. As the gap distance and hole depth changed, the dominant machining mechanism transitioned from EDM to electrochemical discharge machining (ECDM) and ECM. The formation mechanism of the recast layer on nickel alloy was investigated by comparing the surface characteristics of the bulk material and the recast layer using transmission electron microscopy (TEM) and energy-dispersive X-ray spectroscopy (EDS). Comparison experiments with different discharge parameters and sustaining times demonstrated the improved flushing continuity of the working fluid and enhanced discharge gap status achieved by the new flushing systems. Additionally, the application of low voltage and current proved beneficial for the ECM process and the removal of the recast layer.

Wei Chen et al. [6] stated that the occurrence of a short circuit between the tool electrode and the workpiece during electrochemical machining (ECM) can greatly impact process stability, machining efficiency, and the quality of the workpiece surface. Traditional short-circuit detection methods often rely on identifying a large current after the short circuit has already occurred, resulting in burns and damage. This study introduces a new approach that utilizes the polarization voltage characteristic of pulse ECM (PECM) to detect the ECM gap and provide feedback control for the machine tool feed servo. By measuring the polarization voltage during the pulse off time, this method enables early detection of short circuits, thereby preventing burns and improving the stability and efficiency of the ECM process. Additionally, the polarization voltage varies based on the electrolyte characteristics, allowing for adaptable and effective control.

S. Saranya et al. [7] developed a microcontroller-based electrochemical discharge machining (ECDM) setup for drilling quartz substrates in this study. The setup enabled precise fabrication of micro-holes using the constant velocity feed drilling technique. The tool could be moved along the Z-axis with speeds ranging from 1 mm/hr to 50 mm/hr. To evaluate the impact of tool feed rate (TFR) on precision, micro-holes were fabricated at different TFR values between 0.3 $\mu\text{m}/\text{sec}$ and 1.7 $\mu\text{m}/\text{sec}$. The optimal TFR for achieving micro-holes with

the smallest entrance diameter, central diameter, and overcut was determined to be 0.8 $\mu\text{m}/\text{sec}$. Lower TFR values ($< 0.8 \mu\text{m}/\text{sec}$) were employed for creating through-holes on the substrates. Notably, a through-hole with an aspect ratio of 2.32, entrance diameter of 820 μm , and exit diameter of 677 μm was successfully fabricated at a TFR of 0.6 $\mu\text{m}/\text{sec}$.

J. Kozak et al. [8] worked on prototype development of a computer-aided engineering system for the solution of manufacturing problems of ECM such as: tool-electrode design, selection of machining parameters and optimization. The solutions based on computer simulation system had been obtained for different kinds of ECM operations such as EC sinking, EC milling, EC smoothing, ECM-CNC with universal electrode, etc. The analytical type expert system was employed for the selection of electrochemical methods of manufacturing, simulation of different ECM processes for analysing machining conditions and results of machining, recognition and diagnoses for the causes of the trouble in EC-manufacturing and suggestions of some remedies for them. Synthetic type expert system was applied for planning and optimization of condition of selected method of EC-manufacturing, tool-electrode design for ECM, tooling design.

Wenjian Cao et al. [9] studied the application of counter-rotating electrochemical machining (CRECM) for machining thin-walled revolving parts, particularly thin-walled engine cases. The distribution of electric field intensity on the revolving anode surface is non-uniform and challenging to accurately calculate. To address this, a novel equivalent model based on complex variable function was proposed to analytically solve the electric field in CRECM. Additionally, an anode material dissolution model was established for CRECM. The research thoroughly investigated the variations of material removal rate (MRR) and inter-electrode gap (IEG) under different machining parameters. The results revealed that the MRR reached a relative equilibrium state after a transition stage, and this relative equilibrium MRR exceeded the feed rate, resulting in a linear increase in the IEG. Furthermore, numerical optimization of the machining parameters was conducted to minimize the time required to reach the relative equilibrium state. Experimental validation was carried out, and the results aligned well with the theoretical values, demonstrating the effectiveness of the proposed model in predicting the material dissolution process in CRECM.

N.K. Jain et al. [10] described the optimization of three most important ECM process parameters namely tool feed rate, electrolyte flow velocity and applied voltage with an

objective to minimize geometrical inaccuracy subjected to temperature, choking, and passivity constraints using real-coded genetic algorithms. Comparison of the obtained optimization results with the results of past work in this direction shows an improvement in terms of geometrical accuracy.

Y.Ye et al.[11] performed electrochemical micromachining under mechanical motion mode of tool. In the experiments, at first several slots were machined and corresponding performance characteristics were studied and then a circular groove and continuous pattern slots were made using tool movement along required way. On the experiments of simple slots, it was shown that groove width increased with the increment of pulse period and tip distance whereas groove width decreased with the increment of tool moving rate.

Jinxing LUO et al. [12] stated that the stability and quality of the drilling process can be affected by the value and fluctuations of the electrolyte flow rate. This is particularly important when drilling multiple holes, as the distribution and variations of the flow rate among the tube electrodes can impact machining uniformity and stability. To address this issue, an eight-channel flow control system was developed to measure and dynamically regulate the electrolyte flow rate supplied to each individual tube electrode in real-time. The aim was to improve the uniformity of the flow rate and reduce fluctuations during ECD of small holes. The results showed that real-time flow rate control significantly improved hole quality and machining stability compared to unregulated conditions. The constant flow rate helped stabilize the flow field, leading to better hole profiles. The study determined that an electrolyte flow rate of 200 ml/min was acceptable for ECD of small holes based on hole profile analysis. Furthermore, when the eight-channel flow control system was employed for multiple-hole drilling, the uniformity of the electrolyte flow rate among the tube electrodes improved significantly, resulting in a more stable drilling process. Additionally, the maximum feed rate reached 2.40 mm/min in multiple-hole drilling. These findings demonstrated enhanced machining stability and efficiency.

W. Vanderauweraa et al. [13] performed electrochemical milling process in macro range on stainless steel nr. 1.4550 with a 200g/l NaNO₃ solution acting as the electrolyte. In the experimentation, electrode geometry and electrode rotation on the process performance was investigated. In the investigation, material was removed by a tubular tool following a predefined path in a layer-by-layer fashion. In the experimentation, tool electrode was used

hollow shaped and electrolyte flow system was given by two ways ; electrolyte was supplied through the tool to reach electrolyte into the tool work piece interface efficiently and side by side cross flow of electrolyte was given too to remove the sludge. Experiments showed that the best performance in terms of removal rate, surface quality and accuracy was obtained for using a pulsed voltage input. Moreover, inaccuracies due to the tubular electrode shape was overcome by using alternative electrodes which distributed the flushing holes over the entire cross section of the electrode or by decreasing the inner diameter of the tubular electrodes. Total four types geometrical shape was used in this experimentation and corresponding effects were studied.

S. Aravind et al. [14] focused their study on the machining and characterization of micro-holes on a 300 μm thick copper plate using a hollow stainless steel tool with an outer diameter of 250 μm . A unique experimental setup was utilized, which included a customized pulse generator circuit and a closed-loop tool feed circuit incorporating a current-based sensor to maintain a consistent inter-electrode gap during machining. The selected process parameters for machining include voltage, electrolyte concentration, and duty factor. The impact of these parameters on material removal rate, circularity, radial overcut, and taper angle is analyzed using grey relational analysis. Additionally, the statistical significance of the input parameters and their interactions on the output responses was evaluated using analysis of variance. The topography of the machined holes under various experimental conditions was also examined.

Lizhong Xu et al. [15] primarily determined the accuracy of pulsed electrochemical micromachining by the duration of the pulses. Achieving high accuracy typically required an expensive power source with extremely short pulse durations. In this study, a novel electrochemical micromachining method was proposed that utilizes double feedback circuits to address this challenge. The circuit incorporated both a positive feedback circuit and a negative feedback circuit to regulate the pulse duration of the micromachining system. Experimental results demonstrated that increasing the gains of the feedback circuits significantly improved the machining resolution. Using this method, a micro double cure beam was successfully fabricated, achieving nanometer-level accuracy even when using a conventional power source with standard pulse durations.

3.3 OBJECTIVES OF PRESENT RESEARCH WORK :-

From the review of the past literature, it is quite clear that rigorous research work is being carried out to enhance the performance characteristics in Electrochemical Machining processes. The use of controllers to control various process parameters like inter-electrode gap, electrolyte flow and machining current is also depicted clearly. Despite such improvements, ECM setups are very costly and in fact, affordable ECM setups are not available in the market. This aspect poses a barrier, particularly for small-scale industries. From the review of the past literature as well as market research, it is very clear that to date compact-size, lightweight ECM setups are not available in the market.

Keeping these problems in mind, the objective of the research work is to indigenously develop an affordable mini desktop ECM setup having the following features:

- (i) Compact in size
- (ii) Light in weight
- (iii) Portable
- (iv) Very cheap with respect to other commercial machines available in the market.
- (v) User friendly and versatile in behavior
- (vi) Corrosion resistant

3.4 SCOPES OF THE RESEARCH :-

- (i) To develop a mechanical setup in which a hollow tool in an appropriate tool holder can be moved along X,Y and Z - axes. The setup must be very compact, corrosion resistant, light in weight and can be carried from one place to another very easily.
- (ii) To use appropriate motors, drivers and sensors so that the feedback control system works in a very precise manner.
- (iii) To use micro-controller programming and develop an advanced controller with desired specifications so as to facilitate accurate tool movement. The program should be very easily understandable and can be easily modified to be used for various electrochemical processes that can take place in the same mechanical setup.
- (iv) To develop a corrosion resistant electrolyte circulation system having the faculty to deliver both low-pressure and high-pressure electrolytes in the machining zone. The system must maintain the electrolyte concentration within a required level to allow optimized material removal rate. In order to supply clean electrolytes (free from machining products, sludge, etc.) in the machining zone there must be an electrolyte filtration system as well.

Also, the high-pressure electrolyte must be capable of flowing through a narrow path in a hollow tool during the electrochemical drilling process.

(v) To incorporate suitable DC power supply modules for powering the electrodes, workpiece, and other electrical components. In ECM there is always the possibility of sparking and gap short. Hence, the power supply module must have the ability to detect short-circuit in the machining zone and there must be some facility to set the value of the maximum current limit to get protected from gap short condition. Also, modules must be designed to maintain a steady supply voltage for varying current magnitudes.

(vi) To carry out experiments with the prototype in order to estimate the performance of the proposed ECM setup in real life working environment.

To ease the understanding of mini Electrochemical machining setup, all the hardware components used are being classified into 3 groups.

1. Components used for mechanical setup.
2. Components used for developing electrolyte circulation system.
3. Components used for developing motion control.
4. Components used for developing power supply system.

Now, let us consider each group separately.

4.1 COMPONENTS USED FOR MECHANICAL SETUP :-

(i) V-SLOT Aluminium extrusion :

V-slot aluminium extrusion is a high quality linear rail profile with an extremely smooth V-groove on all 4 sides. Its precise, easy to work with and allows us with unlimited design control through its modular nature. V-slot is an improved form of T-slot aluminium extrusion profile as it combines functionality of T-slot with added advantage of linear motion. The dimension of the extrusions used is 20*20 (mm*mm) .



Figure 4.1: V-slot Aluminium extrusion

(ii) Corner Brackets :

The corner bracket is made from high-quality cast iron material. It is used to connect two 20*20 aluminium extrusion pieces in the right angle. With the help of T slotted screws, these corner bracket provides rigidity and strength to the 20*20 extrusion structure. The corner bracket has a slot at both sides, which can accommodate a standard hex bolt of size M4 and by use of T-slotted nuts, the corner bracket can be fastened to the 2020 extrusion.

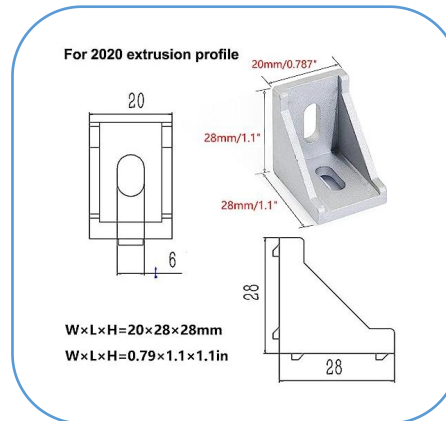


Figure 4.2: Corner bracket with dimensions

(iii) Sliding T-slot Nuts :

T-nuts are used to assemble the frame along with the corner brackets. Their threads are of standard Metric 4 mm (M4) size. These slotted nuts are compatible with the standard 20*20 (mm*mm) aluminium profiles and can be used with standard M4 machine bolts. The nuts have a rough edge on one side making them easier to grip on the inner edge of the aluminium profile. Made from high quality carbon steel, these nuts have high hardness and a long service life. The surface is Nickel-plated for good rust resistance and better performance.



Figure 4.3: Sliding T-nut

The 20*20(mm*mm) Aluminium extrusions, the corner brackets and the sliding T-nuts and M4 bolts are assembled to form a frame to facilitate motion along X,Y,Z axes. A 3D-CAD model of the frame is depicted in figure 4.4. The parts in red are the 3D printed frame mounts.

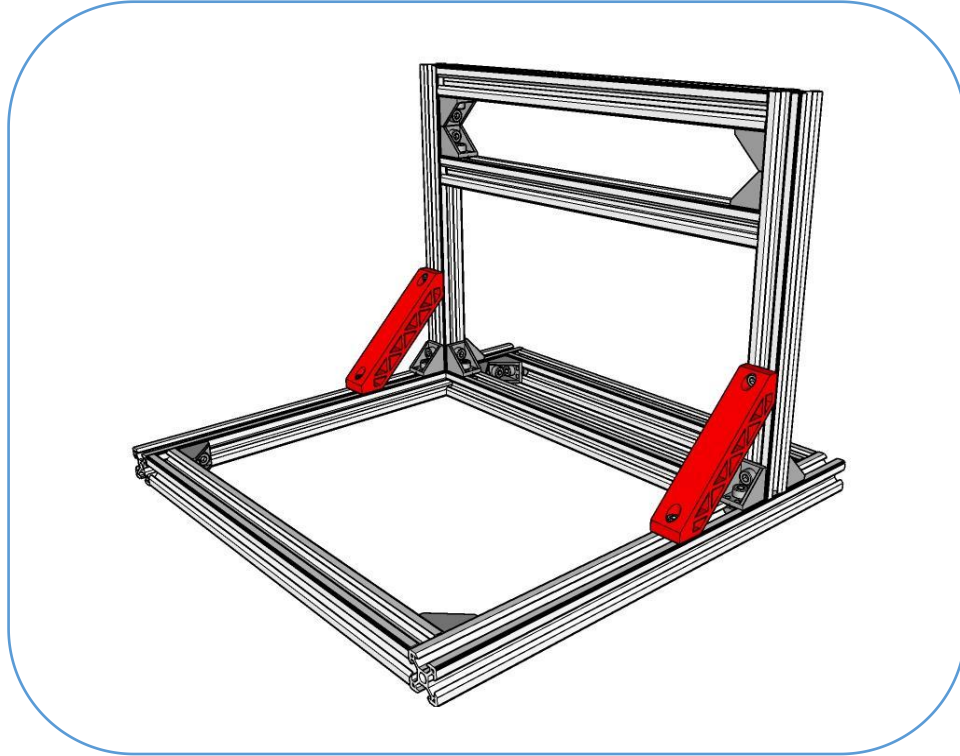


Figure 4.4: CAD model of the frame

(iv) NEMA 17 Stepper Motor :

Even the most basic electronics typically include an electric motor. As a result, it is crucial, particularly in systems that incorporate rotational motion. However, not all engines can be beneficial in circumstances when accuracy is required. The stepper motors are useful in this situation. Stepper motors are brushless direct current (BLDC) motors that divide their rotation into equal steps. A bipolar stepper motor is a type of stepper motor that has a single winding per phase. Bipolar stepper motors are two-phase, four-wire stepper motors. Figure 4.5 shows schematic diagram of bipolar stepper motor.

There are different motors like DC geared motor, servo motor, etc. are available for use in the market but I preferred to use stepper motor in the project because it is a better choice whenever we need any controlled movement. Brushed DC motors rotate continuously when DC voltage is applied to their terminals. Stepper motors are well known for their ability

to transform input pulse trains (usually composed of square waves) into accurate increments in rotational position. Each pulse rotates the shaft through a fixed angle. It is precise and has no any performance loss when the battery voltage drops. There is no lag in performance due to moment of inertia of the motor.

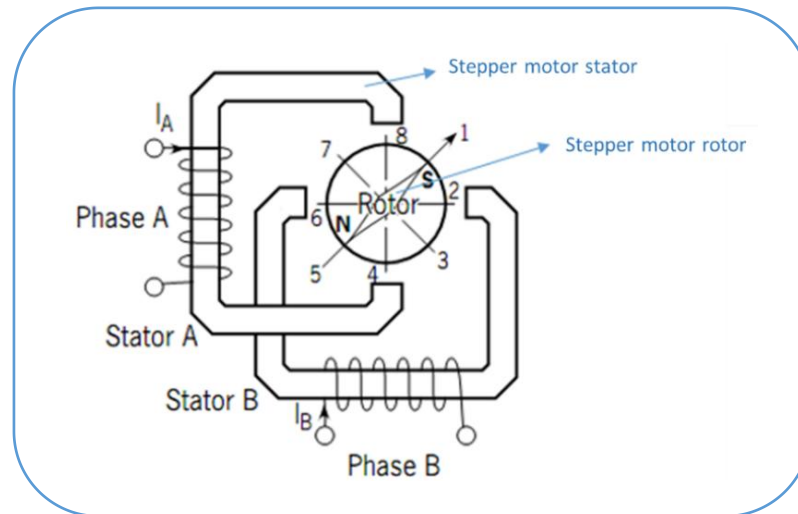


Figure 4.5: Schematic diagram of Bipolar stepper motor

The "NEMA" acronym stands for the National Electrical Manufacturers Association, a distinguished organization that spearheads the establishment of regulations and specifications for diverse models of electric motors. The numerical "17" in NEMA 17 pertains to the square frame size of the motor, a remarkable 1.7 inches, that embodies the standardization of this sought-after stepper motor.



Figure 4.6: NEMA 17 Stepper motor

Physical Specifications of NEMA 17 :

- Frame Size: 42 x 42mm (1.7 inch x 1.7 inch)
- Body Length: 40mm
- Shaft Diameter: 5mm
- Number of Wire Leads: 4
- Wire Length: 400mm
- Weight: 280g
- Temperature rise: 80deg Max(rated current, 2 phase on)

NEMA 17 Stepper motor has a 1.8° step angle. There are 200 steps or revolutions per angle. Each phase of the motor type can draw a voltage of 12V when it is in operation. By changing the rate of the control signal applied, we can easily control the motor speed. Stepper motor can be operated in different step modes such as full step, half step, ¼ step by applying appropriate logic levels to microstep pins of stepper module.

A stepper motor consists of several "toothed" electromagnets arranged as a stator revolving around a central iron rotor as shown in figure 4.7. One electromagnet is powered to magnetically attract the gear teeth and turn the motor shaft. When lined up with the first electromagnet, the gear teeth are slightly offset from the next electromagnet. By turning off one electromagnet and turning on the next, the gear spins a little to line up with the next electromagnet. The process is then repeated. Figure 4.8 shows the schematic diagram of working of stepper motor. In a stepper motor, a full rotation is made up of a number of precise steps, each called a "step".

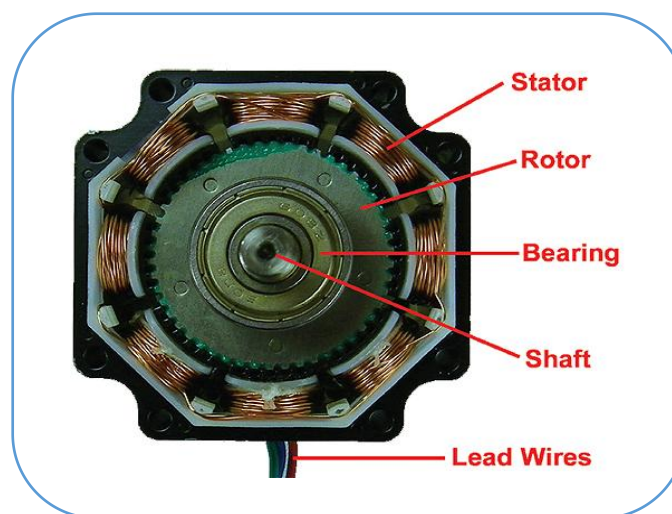


Figure 4.7: Parts of a Stepper motor

Features :

- (i) The input pulse decides the rotation angle of the motor.
- (ii) High accuracy of around 3 to 5% a step.
- (iii) It provides good starting, stopping, and reversing.
- (iv) Control of this motor is less costly because of the exclusion of complex control circuitry.
- (v) The speed is proportional to the frequency of the input pulses.

Electrical Specifications :

- Motor Type: Bipolar Stepper
- Step Angle: 1.8 deg.
- Holding Torque: 40 N.cm (56oz.in)
- Rated Current/phase: 1.7 A
- Phase Resistance: 1.5 Ohm \pm 10%
- Insulation Resistance: 100 M Ω , Min, 500VDC
- Insulation Strength: 500VAC for one minute

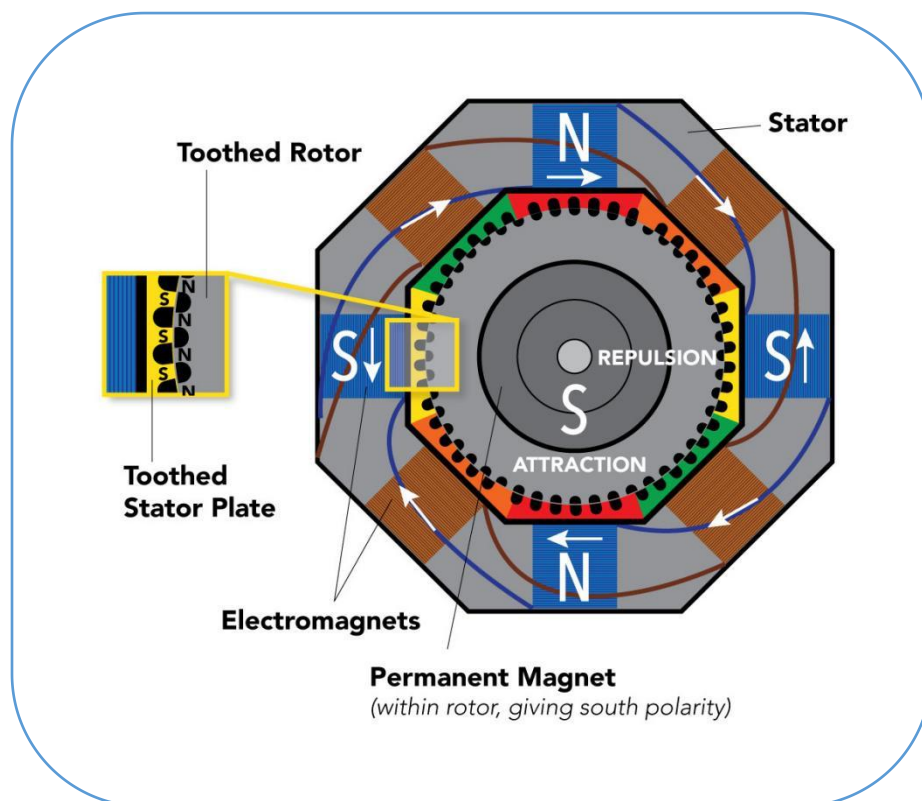


Figure 4.8: Schematic diagram of working of Stepper motor

(v) Trapezoidal Lead Screw :

A lead screw, also known as a power screw or translation screw, is a screw used as a linkage in a machine, to convert rotational motion into translational motion. Because of the large area of sliding contact between their male and female members, screw threads have larger frictional energy losses compared to other linkages. They are not typically used to carry high power, but more for intermittent use in low power actuators and positioner mechanisms. The mechanical advantage of a screw thread depends on its lead, which is the linear distance the screw travels in one revolution. For single start threads, lead equals the pitch of the screw thread. In most applications, the lead is so chosen that the friction is sufficient to prevent linear motion being converted to rotary, that is, the screw does not slip even when linear force is applied, as long as no external rotational force is present.

Trapezoidal thread forms are screw thread profiles with trapezoidal outlines. They are the most common forms used for leadscrews. They offer high strength and ease of manufacture. They are typically found where relatively large loads are handled, as in a vise or the leadscrew of a lathe. Standardized variations include multiple-start threads, left-hand threads, and self-centering threads (which are less likely to bind under lateral forces).

The original trapezoidal thread form, and still probably the one most commonly encountered worldwide, with a 29° thread angle is the Acme thread form. The trapezoidal metric thread form is similar to the Acme thread form, except the thread angle is 30° .

The Stainless steel made trapezoidal leadscrew used has outer diameter (OD) of 8 mm, Length= 300 mm, Lead = Pitch = 2 mm.

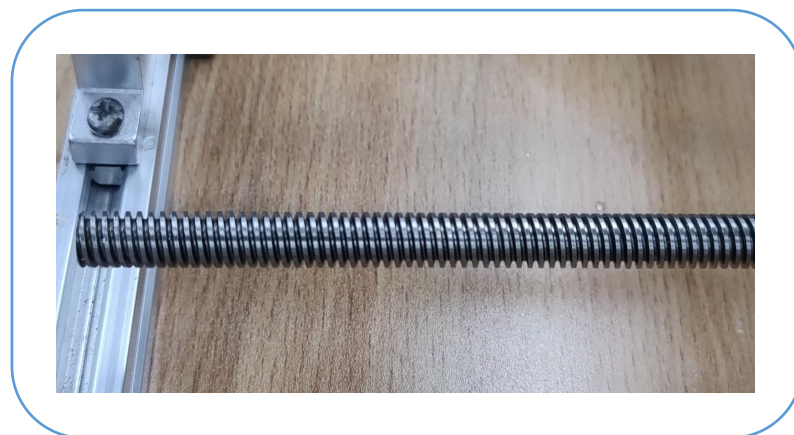


Figure 4.9: T8 Trapezoidal Lead Screw

(vi) Couplings :

A flexible coupling exists to transmit power (torque) from driving shaft to driven shaft. Coupling introduces mechanical flexibility providing misalignment for the shafts. As a result, this coupling flexibility can prevent uneven wear and other mechanical troubles due to misalignment. They can accommodate varying degrees of misalignment up to 1.5° and some parallel misalignment, and in certain cases they provide protective functions such as vibration dampening or acting as a “fuse” in the case of torque overloads. For these reasons, industrial power transmission often calls for flexible rather than rigid couplings.

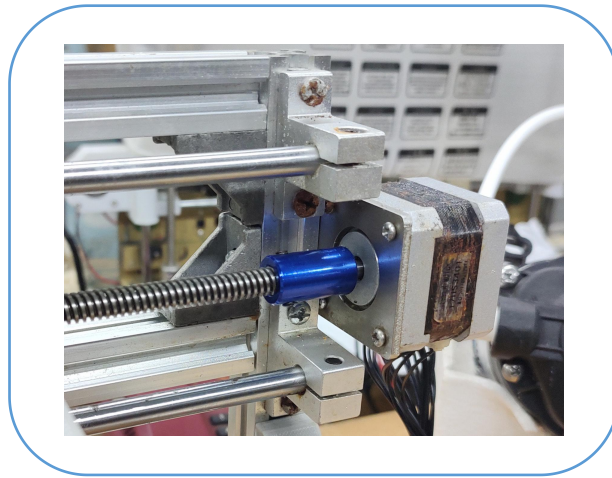


Figure 4.10: Stepper motor coupled with leadscrew

(vii) Chrome plated smooth rods of Stainless steel :

These rods of outer diameter of 8 mm, serve as linear bearings for the X-axis carriage, Z-axis slide (tool holder). They have been chosen for some features as mentioned below:

- High precision, high hardness, high stability.
- Strictly control every precision process to ensure quality.
- Simple design, durable material, high temperature preheat treatment, accurate outer hole size.
- Due to its moderate hardness, it has been applied in many fields.
- Made of stainless steel, high corrosion resistance, high strength and wear resistance to maintain its efficient operation.

(viii) Linear rail bearing support mount SK08 :

SK08 Linear Bearing Support Mount is used mainly to support Smooth Rods of 8 mm outer diameter. These mounts have set screw to secure the smooth rod. This makes mounting and servicing easy. The mount also has 2 x holes on the base to fix it to a base platform. Mounts have high rigidity, high rotating and positioning accuracy.

The assembly of smooth rod and support mount with the frame is shown in figure 4.10.



Figure 4.11: Linear bearing and its supports

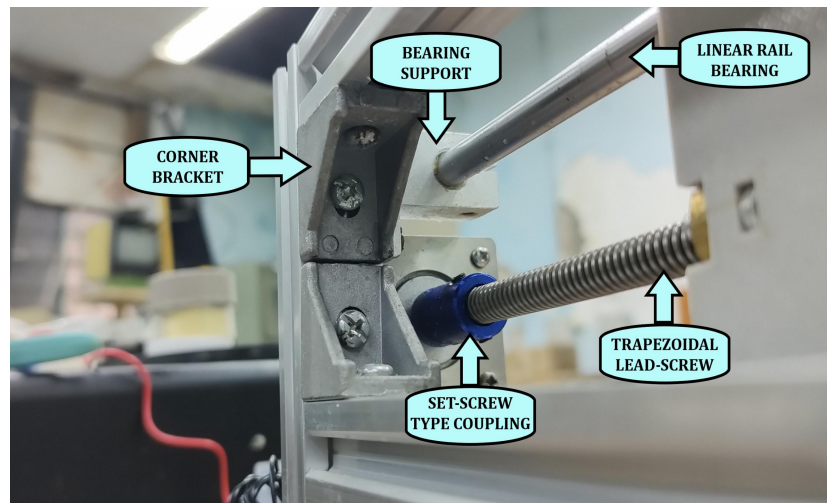


Figure 4.12: Corner brackets and other elements in assembly

(ix) Z-axis Slide and X-axis Carriage :

The 3D-CAD model of Z-axis Slide is shown in figure 4.12. Similarly, the model of X-axis carriage is shown in figure 4.13.

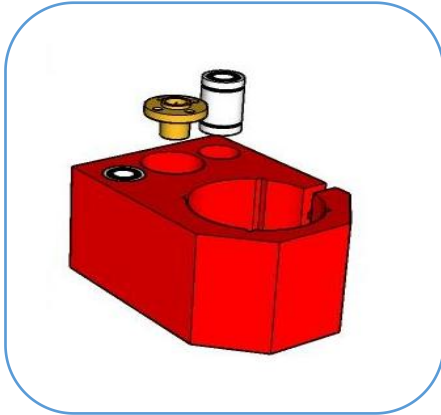


Figure 4.13: Z-axis Slide



Figure 4.14: Linear Bearing

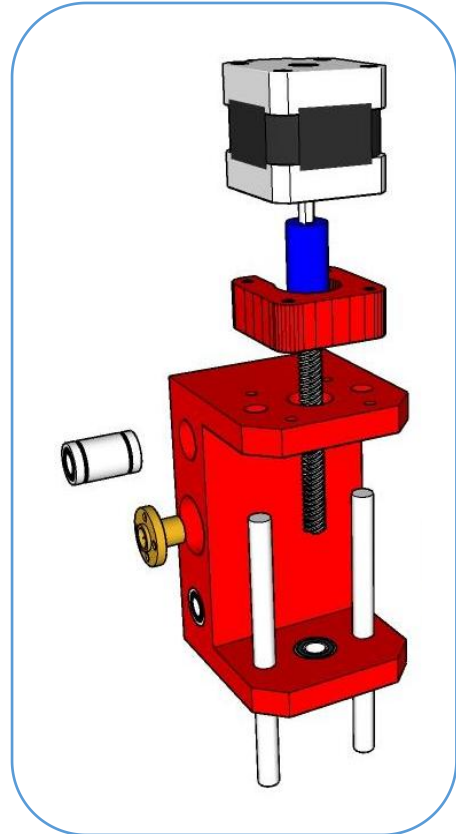


Figure 4.15: X-axis Carriage

The Z-axis Slide is a 3D-printed model. It has a large cylindrical through hole where the tool can be held, and a screw is present to tighten the grip. There are 3 other through holes, one for the trapezoidal leadscrew, and 2 for linear rail bearings. The leadscrew passes through 2 copper screw nuts placed coaxially, thus converting the rotational motion to translational motion of the slide along Z-axis.

Similarly, the X-axis carriage is assembled. The only difference is that, the carriage also houses the stepper motor used for motion along Z-axis. The motor is mounted using 4 motor mounts in the form of cylinders. Screws are used in motor mount assembly. The Slider and the Carriage of the setup are shown in figure 4.15. The assembly of couplings, leadscrews and the linear guides for the aforesaid entities are shown in figure 4.16.

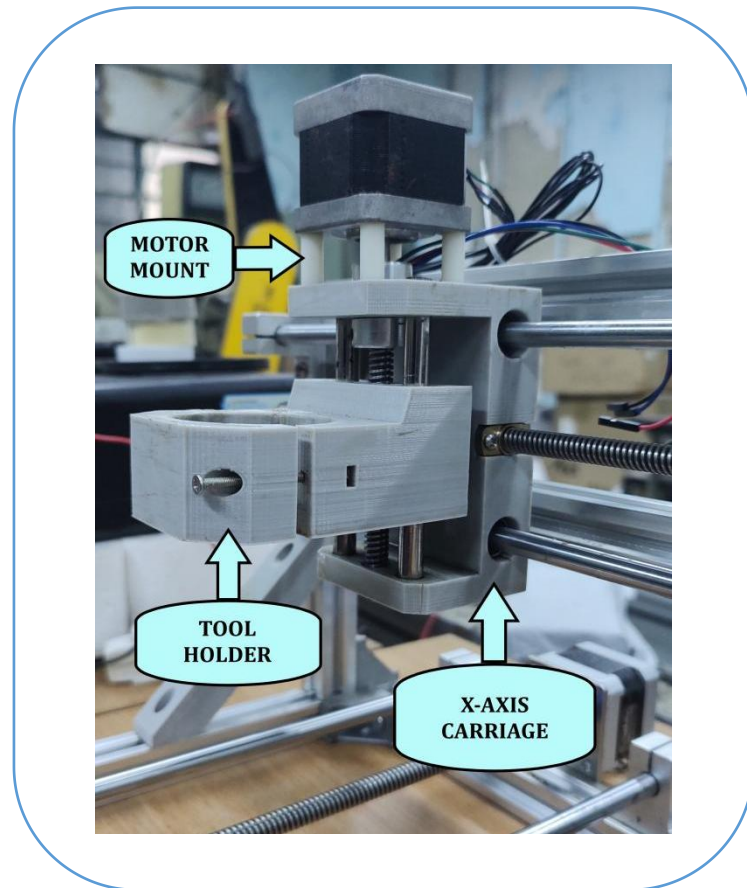


Figure 4.16: Slider and Carriage in the setup

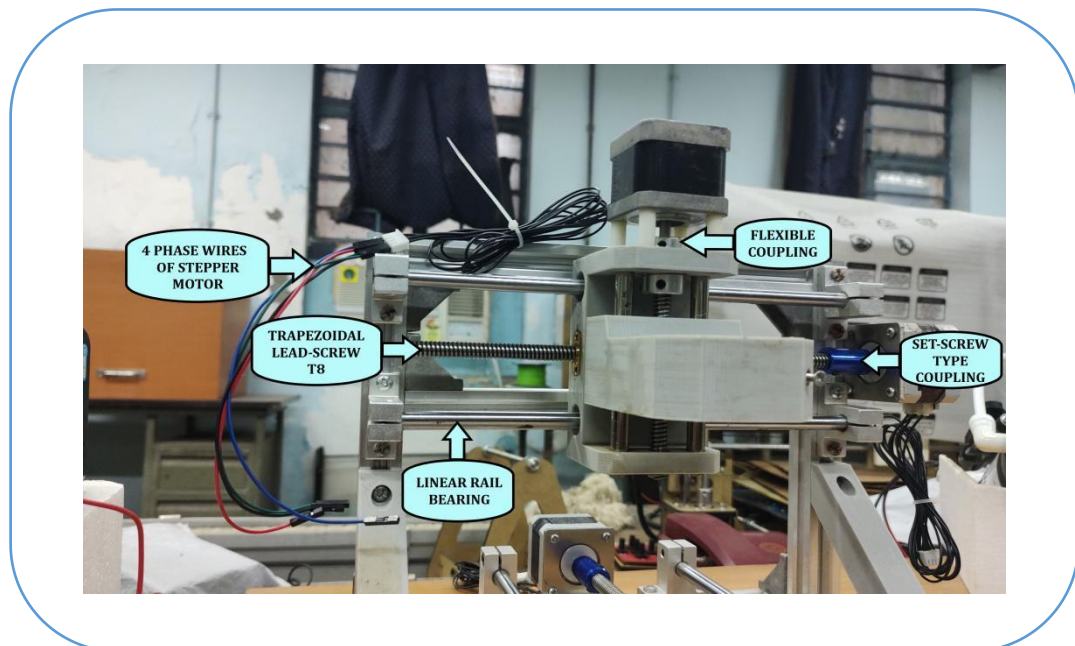


Figure 4.17: X-axis carriage with couplings and leadscrew in assembly

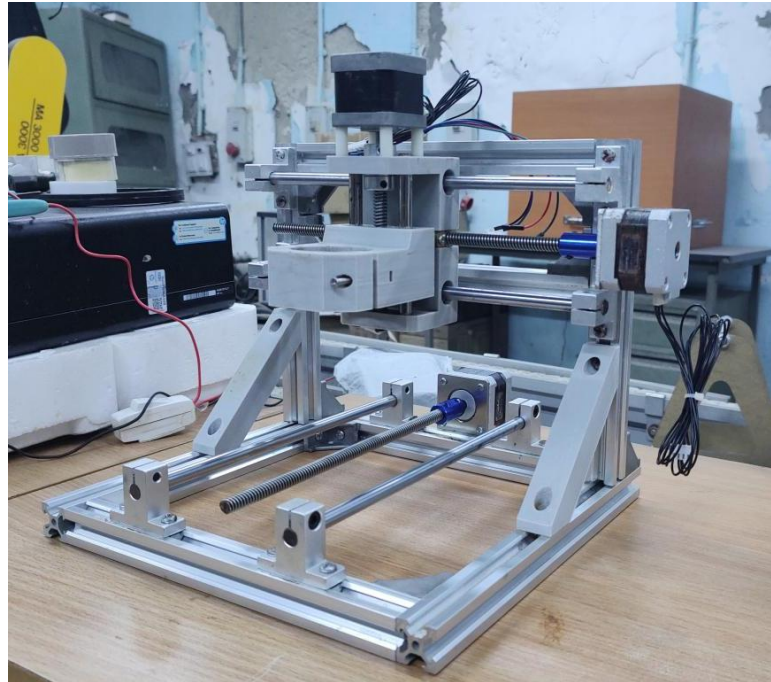


Figure 4.18: The assembled mechanical framework

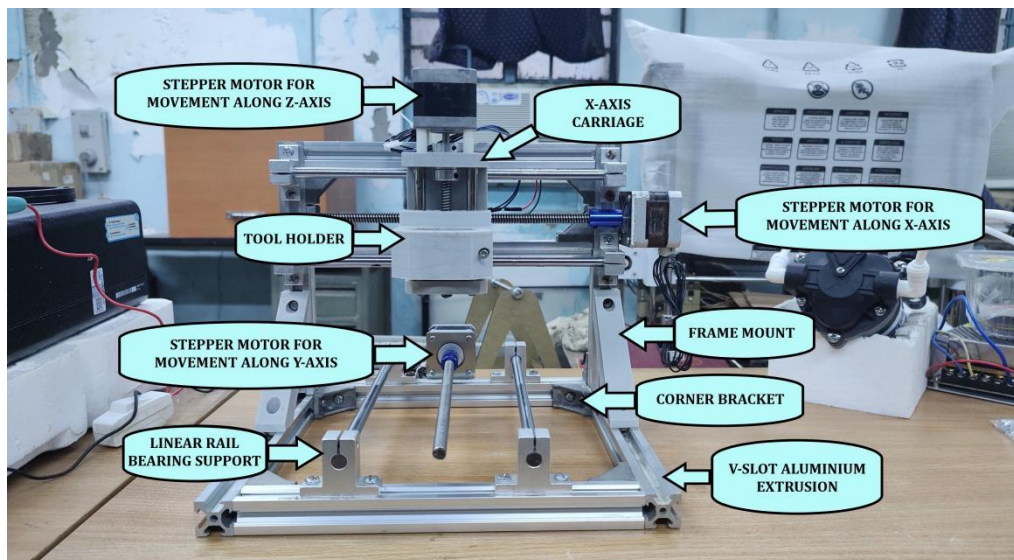


Figure 4.19: Assembled framework with all parts labeled

4.2 COMPONENTS USED FOR DEVELOPING ELECTROLYTE CIRCULATION SYSTEM:-

(i) 12V brush-less submersible centrifugal water pump:

Technical specifications:

- Style: Submersible
- Item dimensions (l*b*h): 7*5*9 (cm*cm*cm)
- Power source: Corded electric
- Item weight: 0.1 kg
- Input DC voltage: 12 V
- Power: 8 W
- H-max: 5 m
- Flow: 10 l/min
- Applications: Used in medical equipments, water cooling system, circulation system.

In a submersible pump the motor is hermetically sealed and close-coupled to the body of the pump. The pump pushes water to the surface by converting rotary energy into kinetic energy into pressure energy. This is done by the water being pulled into the pump, first in the intake, where the rotation of the impeller pushes the water through the diffuser. Submersible pumps are also very efficient because they don't really have to spend a lot of energy moving water into the pump. Water pressure pushes the water into the pump, thus saving a lot of energy. The main advantage of using this pump lies in the fact that all its parts are non-metallic and the motor is sealed, hence corrosive nature of the electrolytes will not be a threat to its longevity. A plastic box will serve as electrolyte holder in the setup, the submersible pump will be placed in it as shown in figure 4.20.

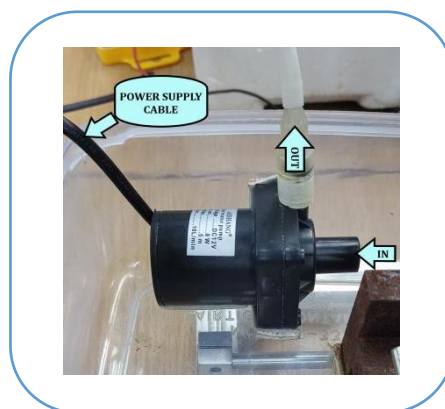


Figure 4.20: Submersible pump in the setup

(ii) 5 micron spun filter with filter housing :

Process filtration is a critical activity for many industrial or manufacturing organisations. The effectiveness of solid separation has impacts on downstream processes and can determine quality standards. A filter removes solid contaminants by capturing and retaining these particles as they pass through the filter media. Filters can consist of many different materials, and they are presented in different formats, such as cartridges, bags and sheets. Each of these consumable filters fit within a permanent housing or vessel. Cartridges are often the most popular format of filter. Spun Filter is made of fine melted polypropylene, which is blown and spun in a cylinder-like form. The micron rating is the size at which particles are retained by the filter. For example, a five-micron filter will stop particles of five microns or larger from passing through the media.

In this application, the main function of the 5 micron spun filter is sludge removal, else the narrow passage in the hollow tool can be clogged leading to decrease in electrolyte pressure. To ensure proper functioning,

RO tubing made of polypropylene having diameter of $\frac{1}{4}$ th of an inch are used to connect the components in circulation system. Input and output terminals of the components are connected with the pipe by threaded polypropylene elbow connector and push fit type elbow connector of $\frac{1}{4}$ th inch inner diameter.



Figure 4.21: Spun filter housing

(iii) 24V Booster diaphragm pump :

A diaphragm pump is a positive displacement pump which can transfer liquids with low, medium or high viscosity and also liquids with a large solids content. A booster pump typically contains a diaphragm, a power supply and a tank pressure switch. The pump uses reciprocation in a diaphragm made of rubber or plastic to pump water from an intake to an outtake. The diaphragm works in cooperation with valves on both sides to increase the pressure of liquid as it flows through the pump. These pumps can handle difficult fluids such as corrosive chemicals, dirty water, abrasive slurry and volatile solvents.

Generally there is a pressure drop of the electrolyte when it passes through spun filter. This low pressure electrolyte is not quite functional to clean out the sludges trapped in the machining zone during deep hole drilling thereby leading to errors in motion control and hole quality. To add on to the advantage of using this pump, it must be told that greater the pressure of the electrolyte, greater and effective will be its filtration rate.

Technical specifications :

- Input current rating: 24 V, 1.2 A
- Flow rate: 1.8 l/min
- Maximum pressure developed: 110 Psi

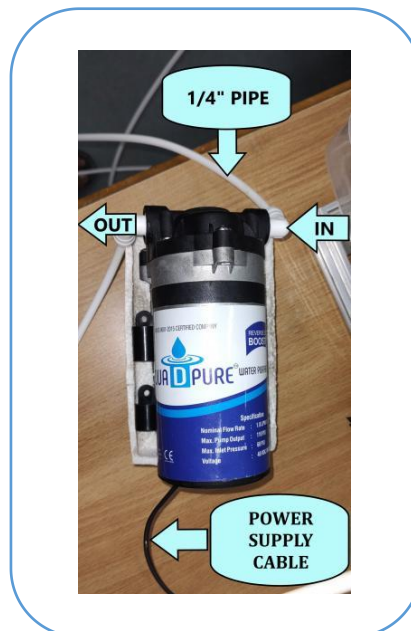


Figure 4.22: Booster pump in the setup

4.3 COMPONENTS USED FOR DEVELOPING MOTION CONTROL :-

(i) Arduino NANO having micro-controller ATmega328P :

The main microcontroller used to control the machining is ATmega328P of the AVR family. It can be considered as the brain of the ECM setup. AVR is a family of microcontrollers developed since 1996 by Atmel, acquired by Microchip Technology in 2016. These are modified Harvard architecture 8-bit RISC single-chip micro-controllers. AVR was one of the first microcontroller families to use on-chip flash memory for program storage, as opposed to one-time programmable ROM, EPROM, or EEPROM used by other micro-controllers at the time.

AVR micro-controllers find many applications as embedded systems. They are especially common in hobbyist and educational embedded applications, popularized by their inclusion in many of the Arduino line of open hardware development boards.

There are many micro-controllers like PLC series, AVR series, 8051, raspberry, etc. available in the market, but I have selected the Arduino microcontroller board because it comes with a complete package which includes 5V regulator, an oscillator, a microcontroller, serial communication interface, LED, a buzzer and headers for the connection, which makes it very easy in use and very simple to assemble components with it.

The Arduino Nano is Arduino's classic breadboard friendly designed board with the smallest dimensions. The Arduino Nano comes with pin headers that allow for an easy attachment onto a breadboard and features a Mini-B USB connector.

It is an open source prototyping platform i.e. the board can be easily modified and optimized for better functionality. It has no power plug for external power supply. It is smaller in size and less in weight than the Arduino UNO. The Arduino Nano is equipped with 30 male I/O headers, in a DIP-30-like configuration, which can be programmed using the Arduino Software integrated development environment (IDE), which is common to all Arduino boards and running both online and offline. The board can be powered through a type-B mini-USB cable or from a 9 V battery.

Technical specifications of Arduino NANO:

- Microcontroller: 8-bit AVR Micro-controller ATmega328P
- Operating voltage: 5 volts
- Input voltage: 5 to 20 volts

- Digital I/O pins: 14 (6 optional PWM outputs)
- Analog input pins: 8
- 6 channel 10 bit A/D convertors
- DC per I/O pin: 40 mA
- DC for 3.3 V pin: 50 mA
- Flash memory: 32 KB, of which 2 KB is used by bootloader
- SRAM: 2 KB
- EEPROM: 1 KB
- Clock speed: 16 MHz
- Length: 45 mm
- Mass: 7 g
- USB: Mini-USB Type-B
- ICSP Header: Yes
- DC Power Jack: No
- Two 8-bit timers with separate prescaler and compare mode.
- One 16-bit timer separate prescaler, compare and capture mode.

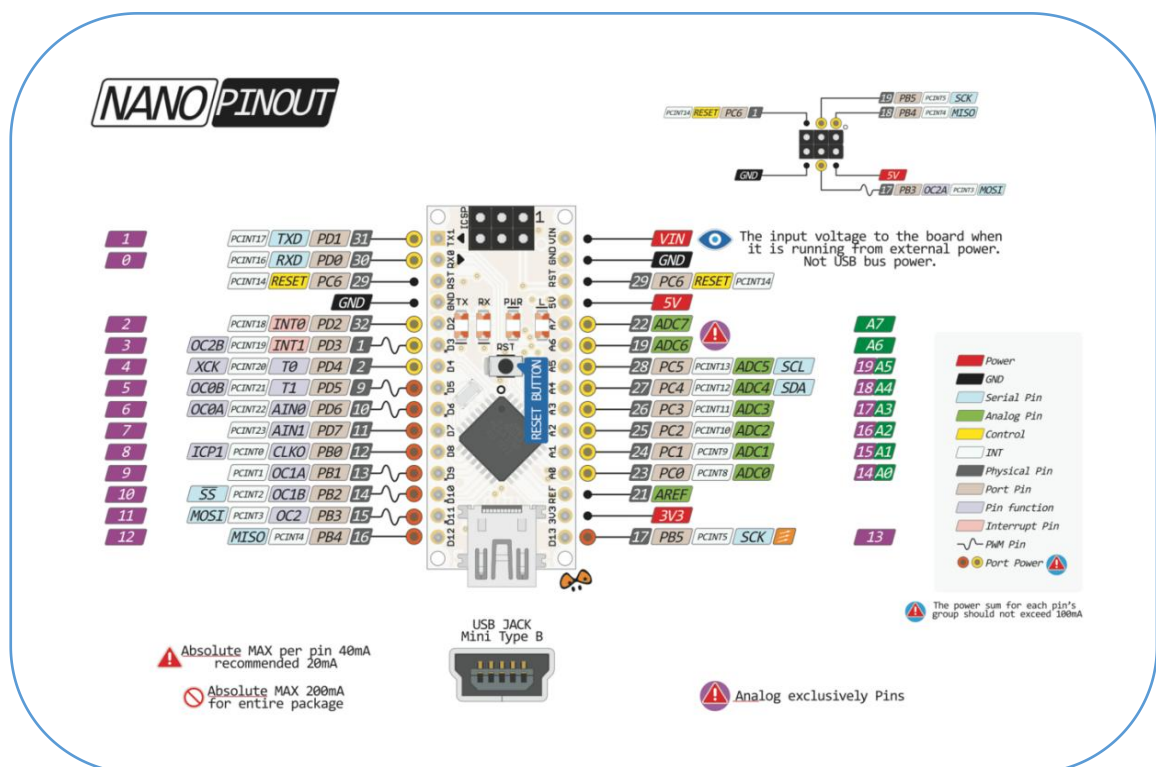


Figure 4.24: Arduino NANO pin description

(ii) Hall Effect Base Linear Current sensor WCS1700 :

An electronic device which converts magnetic or magnetically encoded data into electrical signals is called a Hall effect sensor. It is a solid-state device that is turning out to be increasingly more well known in view of its multi-purposes in various sorts of utilization. Hall Effect sensors are insusceptible to vibration, residue(dust) and water. The sensor is a slim fragment of semiconductor material very much like the chip inside a RAM device.

Principle of Hall effect - The principle of the Hall effect states that when a current-carrying conductor or a semiconductor is introduced to a perpendicular magnetic field, a voltage can be measured at the right angle to the current path. This effect of obtaining a measurable voltage is known as the Hall effect.

Theory - When a conductive plate is connected to a circuit with a battery, then current starts flowing. The charge carriers will follow a linear path from one end of the plate to the other end. The motion of charge carriers results in the production of magnetic fields. When a magnet is placed near the plate, the magnetic field of the charge carriers is distorted. This upsets the straight flow of the charge carriers. The force which upsets the direction of flow of charge carriers is known as Lorentz force. Due to the distortion in the magnetic field of the charge carriers, the negatively charged electrons will be deflected to one side of the plate and positively charged holes to the other side. A potential difference, known as the Hall voltage will be generated between both sides of the plate which can be measured using a metre.

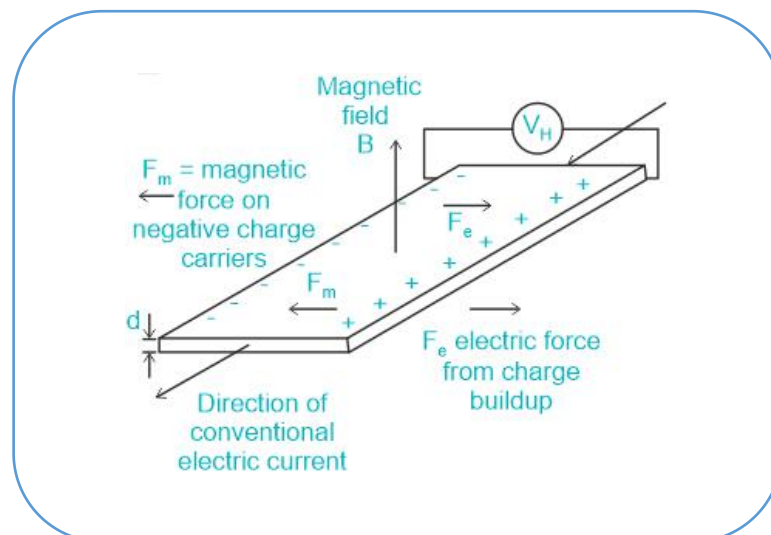


Figure 4.25: Conductor developing potential difference due to Lorentz force

The Winsen WCS1700 current sensor provides economical and precise solution for both DC and AC current sensing in industrial, commercial and communications systems. Typical applications include motor control, load detection and management, over-current fault detection and any intelligent power management system etc. The WCS1700 consists of a precise, low-temperature drift linear hall sensor IC with a temperature compensation circuit and through-hole of 9.0 mm². Users can use system's own electric wire by passing it through this hole in the sensor to measure passing current as shown in figure 4.26. This design allows system designers to monitor any current path without breaking or changing original system layout at all. Any current flowing through this hole will generate a magnetic field which is sensed by the integrated Hall IC and converted into a proportional voltage (linear with the magnetic flux density). The terminals of the conductive path are electrically isolated from the sensor leads. This allows the WCS1700 current sensor to be used in applications requiring electrical isolation without the use of opto-isolators or other costly isolation techniques and make system more competitive in cost. Capacitor C (0.01uF~0.1uF) is recommended to be connected between V_{out} and ground to reduce output noise. Response of the sensor is sent to the arduino its analog output pin. The sensor module used in the setup is shown in figure 4.27.

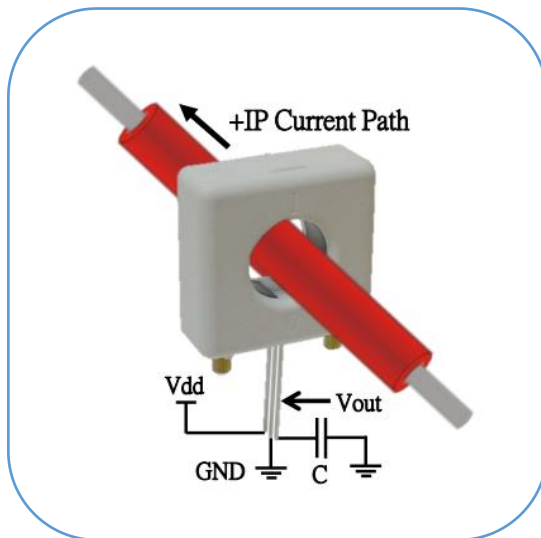


Figure 4.26: Wire through sensing unit



Figure 4.27: WCS 1700 Sensor Module

Features:

- Wide sensing current range: 0 ~ 70 A at 5 V.
- High sensitivity of 33 mV/A and low operating current of 3 mA .
- Wide operating voltage range: 3 ~ 12 V.

(iii) Stepper motor driver DRV8825 :

The DRV8825 from Texas Instruments, is a micro-stepping driver for controlling bipolar stepper motors which have a built-in translator for easy operation. Due to the simplicity of the stepper motor control and the variety of stepping modes provided by the driver, it is an ideal solution for building applications that require precise and reliable motor control, such as the movement control of beds, heads, and assemblies in various CNC machines, 3D printers, Automated Teller Machines, etc.

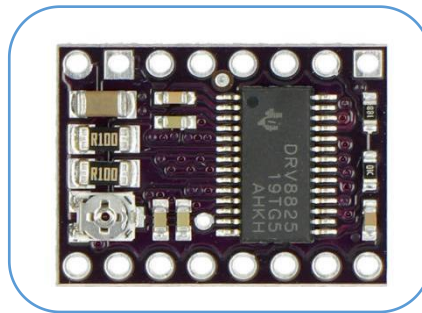


Figure 4.28: DRV8825 Sensor Module

The DRV8825 stepper motor driver has output drive capacity of up to 45V. This allows us to control a bipolar stepper motor, such as the NEMA 17, at up to 2.5A maximum current and up to 1A continuous current, per coil. Furthermore, the output current is regulated, allowing for noiseless operation of the stepper motor and the elimination of resonance that is common in unregulated driver designs. The driver offers six different step resolutions: full-step, half-step, quarter-step, eighth-step, sixteenth-step, and thirty-second-step. In order to ensure reliable operation, the driver has additional features such as under-voltage, shoot-through, short circuit, overcurrent, and thermal protection.

Another stepper motor driver widely accepted among users is A4988, but it has some important differences in comparison to DRV8825. Following are the points of difference that explain why I have preferred to use DRV8825 in my setup :

- The DRV8825 offers 1/32-step micro-stepping while the A4988 only goes down to 1/16-step.
- The DRV8825 has a higher maximum supply voltage(45 V) than the A4988 (35 V), which means the DRV8825 can be used more safely at higher voltages and is less susceptible to damage from Inductance-capacitance (LC) voltage spikes.
- The DRV8825 can deliver more current than the A4988 without any additional cooling.

The DRV8825 sensor module has a total of 16 pins that connect it to the outer world.

Figure 4.29 shows the pinout diagram of the module.

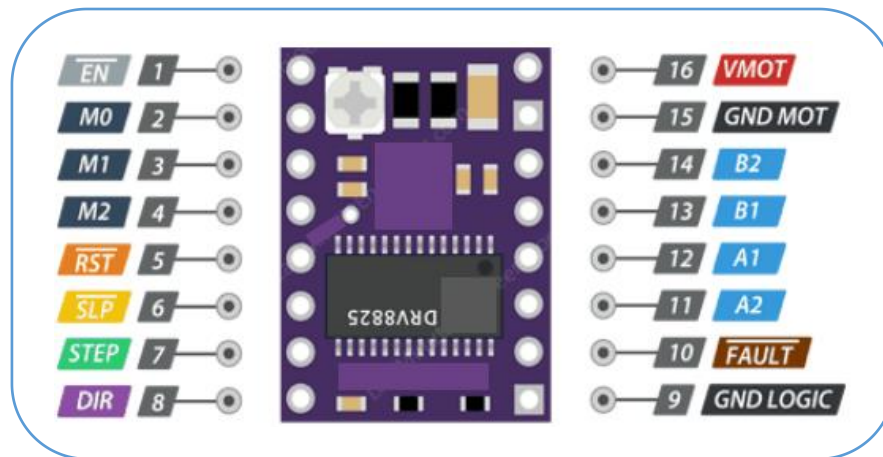


Figure 4.29: Pinout diagram of DRV8825 module

Power pins:

VMOT (Voltage for Motor) supply power to the motor. Any voltage between 8.2V and 45V can be connected to this pin from a dedicated power supply.

GND MOT (Ground of Motor) is the ground terminal for the motor's power supply, and should be connected to the negative terminal of the dedicated power supply.

The module doesn't have a logic supply pin because the DRV8825 draws its power from the motor power supply using an internal 3V3 (3.3 Volt) voltage regulator. However, the microcontroller's Ground pin should be connected to the **GND LOGIC** (Logic Ground) pin.

Microstep selection pins:

The DRV8825 driver supports microstepping by dividing a single step into smaller steps. This is achieved by energizing the coils with intermediate current levels. For example, if we choose to drive the NEMA 17 (200 steps per revolution in full-step mode) in quarter-step mode, the motor will produce 800 microsteps per revolution.

The DRV8825 driver has three step size selector inputs: **M0** (MODE 0), **M1** (MODE 1) and **M2** (MODE 2). By setting the appropriate logic levels for these pins, we can set the motor to one of six step resolutions. These three microstep selection pins are pulled low by on-board

pull-down resistors, so if we leave them unconnected, the motor will operate in full-step mode. The logic level combinations required for various step resolutions are shown in table 4.1 .

<u>M0</u>	<u>M1</u>	<u>M2</u>	<u>Microstep Resolution</u>
Low	Low	Low	Full step
High	Low	Low	Half step
Low	High	Low	1/4 step
High	High	Low	1/8 step
Low	Low	High	1/16 step
High	Low	High	1/32 step
Low	High	High	1/32 step
High	High	High	1/32 step

Table 4.1: Logic level combinations for the step resolutions

Control Input pins:

The DRV8825 has two control inputs: **STEP** and **DIR**.

STEP input controls the microsteps of the motor. Each HIGH pulse sent to this pin drives the motor according to the number of microsteps determined by the microstep selection pins. The higher the pulse frequency, the faster the motor will spin.

DIR input controls the spinning direction of the motor. Pulling it HIGH turns the motor clockwise, while pulling it LOW turns it counterclockwise. If we want the motor to turn only in one direction, we can either connect the DIR directly to 5V pin or Ground pin of the microcontroller board.

Pins for controlling Power States:

The DRV8825 has three separate inputs for controlling its power states: **EN** (ENABLE), **RST** (RESET), and **SLP** (SLEEP).

EN (ENABLE) is an active low input pin. When this pin is pulled LOW, the DRV8825 driver is enabled. By default, this pin is pulled low, so unless it is pulled high, the driver is always enabled. This pin is particularly useful when implementing an emergency stop or shutdown system.

SLP (SLEEP) is an active low input pin. Pulling this pin LOW puts the driver into sleep mode, reducing power consumption to a minimum. This pin can be used to save power, especially when the motor is not in use.

RST (RESET) is an active low input as well. When this pin is pulled LOW, all STEP inputs are ignored. It also resets the driver by setting the internal translator to a predefined “home” state. Home state is basically the initial position from which the motor starts, and it varies based on microstep resolution.

Fault Detection Pin:

The DRV8825 has a **FAULT** output that drives LOW whenever the H-bridge Field Effect Transistors (FETs) are disabled as the result of over-current protection or thermal shutdown. The FAULT pin is typically shorted to the SLEEP pin, therefore, whenever the Fault pin is driven LOW, the entire chip is disabled. And it will remain disabled until it is either RESET or Motor Voltage VMOT is removed and reapplied.

Output Pins:

The output channels of the DRV8825 motor driver are broken out to the side of the module with pins **B2**, **B1**, **A1** and **A2** pins. Any small to medium-sized bipolar stepper motor, such as NEMA 17, can be connected to these pins.

Each output pin can supply up to 2.5A to the motor. The amount of current supplied to the motor, however, depends on the power supply, cooling system, and current limiting setting of the system. Despite having a maximum current rating of 2.5A per coil, the DRV8825 driver IC can only supply about 1.5A per coil without overheating. To achieve more than 1.5A per coil, a heat sink or other cooling method is required.

Current limiting:

Before running the motor, the maximum current flowing through the stepper coils should be limited so that it does not exceed the motor's rated current. The DRV8825 driver includes a small trimmer potentiometer for setting the current limit.

Here, the method of measuring the reference voltage (V_{ref}) at the potentiometer has been used. Firstly, the datasheet of the stepper motor is checked for knowing the rated current. In this setup, the stepper motor (NEMA 17) has rated current of 12V and 350 mA. Now, the microstep pins (M0, M1, M2) are disconnected and the driver is enabled in full step mode. The motor is held in a fixed position without clocking the step input. Then, the voltage on the potentiometer is continuously measured and it is rotated very slowly trying to adjust the voltage according to the formula -

$$V_{\text{ref}} = \text{current limit} / 2$$

Sudden rotations of potentiometer should be avoided while driver is in operation, as this generates huge heat and destroys the IC.

Wiring a DRV8825 Stepper Motor Driver to an Arduino:

The connections are straightforward. The RST pin is connected to the adjacent SLP pin and 5V on the Arduino to keep the driver enabled. The GND LOGIC pin to the Arduino's ground pin. The DIR and STEP input pins are connected to the Arduino NANO's digital output pins D2 and D3. The stepper motor connects to the B2, B1, A1, and A2 pins of DRV8825. 'A' stands for coil on Stator A and 'B' stands for coil on Stator B. The pins of the same coil can be found out easily. Firstly, any two of the four pins on the motor are short-circuited. If it is noticed that the motor shaft rotation is tough, then it is understood that pins of the same coil are short-circuited. Actually, the DRV8825 module is conveniently laid out to match the 4-pin connector on bipolar stepper motors, so that shouldn't be a problem. Then, the microstep resolution pins namely M0, M1, M2 and SLP, RST pins are connected to the 5V pin as per the requirements. Finally, the motor power supply to the VMOT and GND MOT pins are connected. A large 100 μ F decoupling electrolytic capacitor may be put across the motor power supply pins to avoid large voltage spikes.

4.4 COMPONENTS USED FOR DEVELOPING POWER SUPPLY SYSTEM :-

(i) Switched Mode Power Supply (SMPS) :

A switched-mode power supply (SMPS) is an electronic circuit that converts power using switching devices that are turned on and off at high frequencies, and storage components such as inductors or capacitors to supply power when the switching device is in its non-conduction state. Switching power supplies have high efficiency and are widely used in a variety of electronic equipment, including computers and other sensitive equipment requiring stable and efficient power supply. In the SMPS device, a switching regulator is used which switches on and off the load current to maintain and regulate the voltage output. Suitable power generation for a system is the mean voltage between off and on modes. Unlike the linear power supply, the SMPS carry transistor switches among low dissipation, full-on and full-off phase, and spend much less time in high dissipation cycles, which decreases depleted strength. The SMPS is mostly used where switching of voltages is not at all a problem and where efficiency of the system really matters.

There are few points which are to be noted regarding SMPS. They are,

- SMPS circuit is operated by switching and hence the voltages vary continuously.
- The switching device is operated in saturation or cut off mode.
- The output voltage is controlled by the switching time of the feedback circuitry.
- Switching time is adjusted by adjusting the duty cycle.
- The efficiency of SMPS is high because, instead of dissipating excess power as heat, it continuously switches its input to control the output.

There are few disadvantages in SMPS, such as

- The noise is present due to high frequency switching.
- The circuit is complex.
- It produces electromagnetic interference.

The advantages of SMPS include,

- Low DC ripple efficiency is as high as 80 to 90%
- Less heat generation hence less power wastage.
- Reduced harmonic feedback into the supply mains.
- Over-Voltage Protection: When output voltage is greater than 130-140% of rated voltage, the supply turns off.

- Over-Load Protection: When load power is greater than 130-140% of rated power, it triggers protection function.
- Short-circuit Protection: When output terminal is short-circuited, it turns off output.
- Over-Current Protection: When output current is greater than 115-130% of the rated current, the output voltage begins to drop.
- High-Temperature Protection: It automatically protect the power supply when there is high temperature.



Figure 4.30: SMPS module

Three different power supply modules have been used in the setup and their terminal connections with other electrical components are described below:

- SMPS 1 supplies power for electrochemical machining. It has rated power of 400 W and regulated output voltage of 60 V. Maximum rated current output is 6.67 A. The anode (workpiece) connects to positive terminal and the cathode (tool) connects to the negative terminal.
- SMPS 2 has rated power of 120 W and regulated output voltage of 12 V. Maximum rated current output is 10 A. It supplies power to the submersible pump, VMOT pin of the DRV8825 and the positive input terminal of buck converter. Similarly, the negative terminal of SMPS connects to the ground terminal of the pump, negative output terminal of buck converter and GND pin of DRV8825.

Buck converter is a DC-to-DC converter which steps down the input voltage to 5 V. It operates on the same principle as that of a SMPS. It's positive output terminal provides the regulated 5 V input to Arduino NANO using VIN pin, and to the sensor WCS1700. The GND terminals of current sensor and Arduino NANO are connected to the negative output terminal of the buck converter.

- SMPS 3 has rated power of 240 W and regulated output voltage of 24 V with maximum rated current of 10 A. It is used for supplying power to the booster pump in the setup.

The network of electrical connections among all the components and modules used for developing the electrochemical machining setup is shown below in figure 4.31. The connections are labeled. The power supplies have been marked numerically according to the above mentioned explanations.

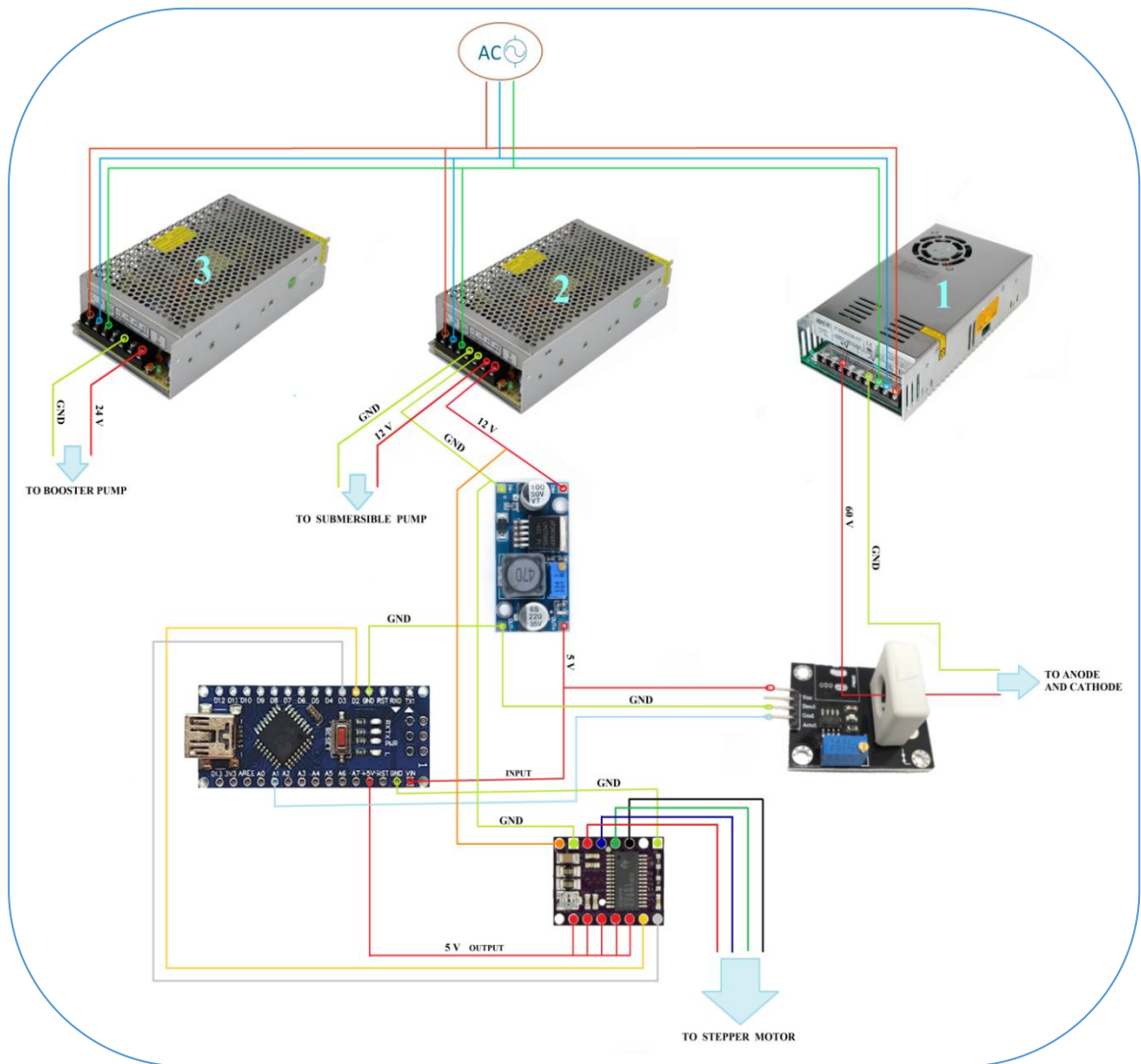


Figure 4.31: Schematic connection diagram of the components

5.1 INTRODUCTION :-

The most widely used high-level language for AVR microcontrollers. AVR-GCC is a compiler that takes C language high level code and creates a binary source which can be uploaded into an AVR microcontroller. 8-bit AVR microcontrollers are commonly programmed using C. Because these devices have small program memories, C compiler optimization is usually enabled. This causes some lines of C code to be optimized away or to be combined with other lines of code.

PID control stands for proportional–integral–derivative control which is a closed-loop feedback mechanism used in a control system. This type of control is also termed as three-term control. By calculating and controlling the actuating signal summed up of three parameters – the proportional, integral and derivative of how much a process variable deviates from the desired set point value (this deviation is termed as error)– we can achieve different control actions for specific work. PID controllers are considered to be the best controllers in the control system family. Nicholas Minorsky published the theoretical analysis paper on PID controller.

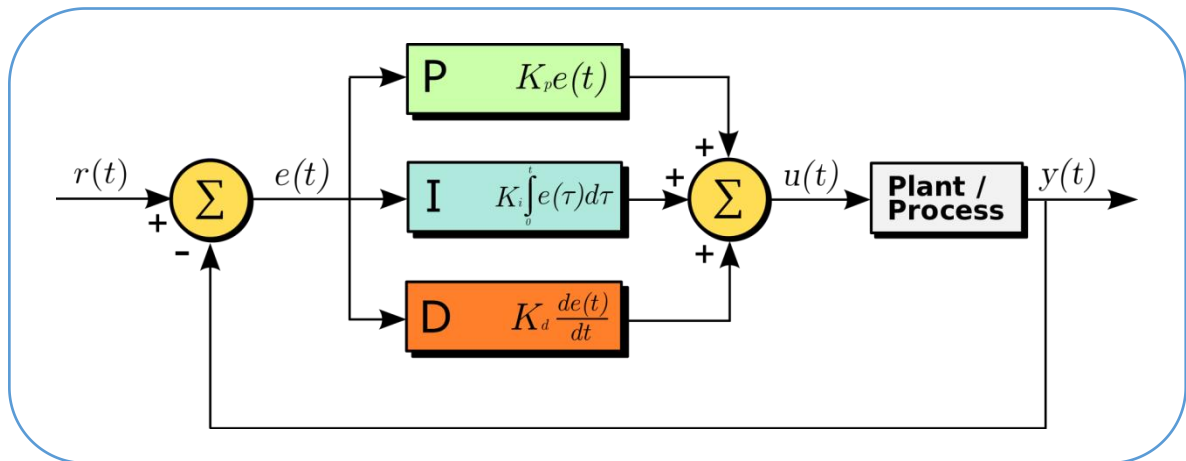


Figure 5.1: Block diagram of PID controller

In the block diagram of the closed loop system shown above, $r(t)$ represents the desired set point value (SP), $y(t)$ represents the process variable (PV), $e(t)$ represents the error between SP and PV, $u(t)$ is the actuating signal or control variable of the process. The control algorithm tries to minimize the error over time by adjusting the control variable.

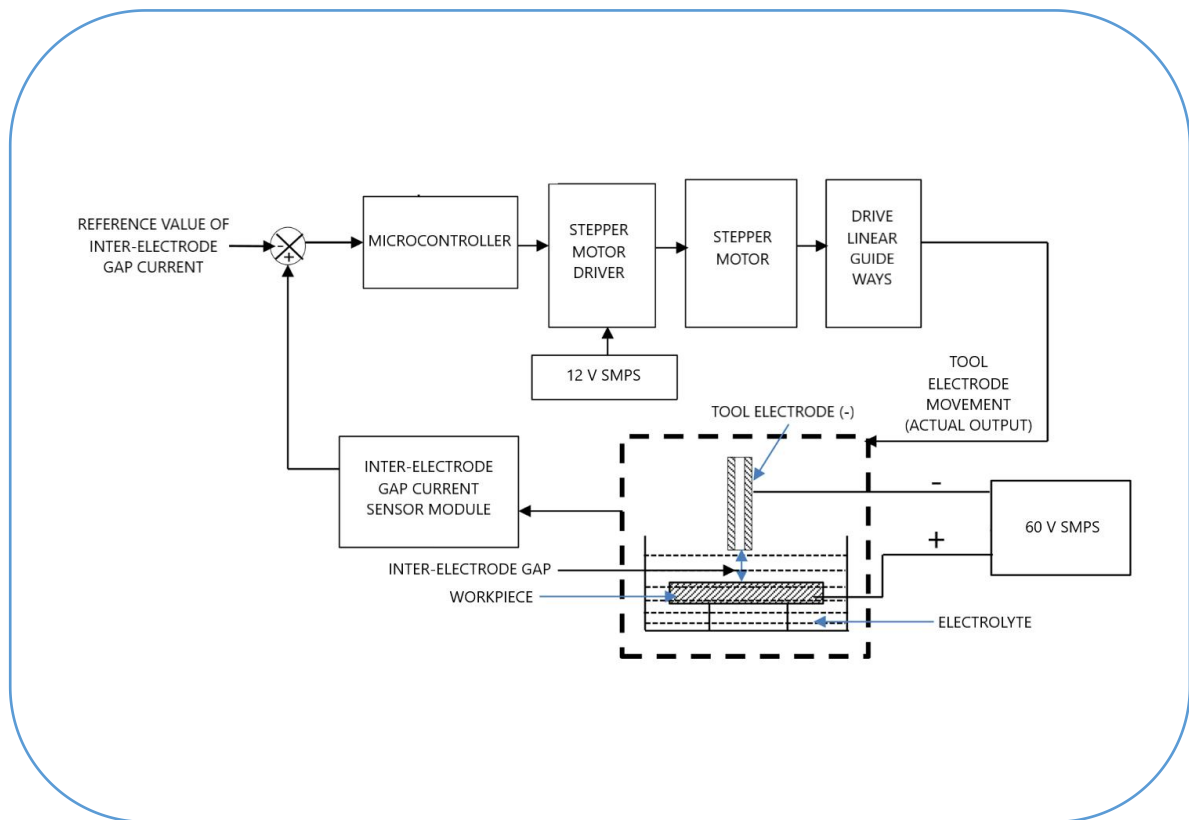
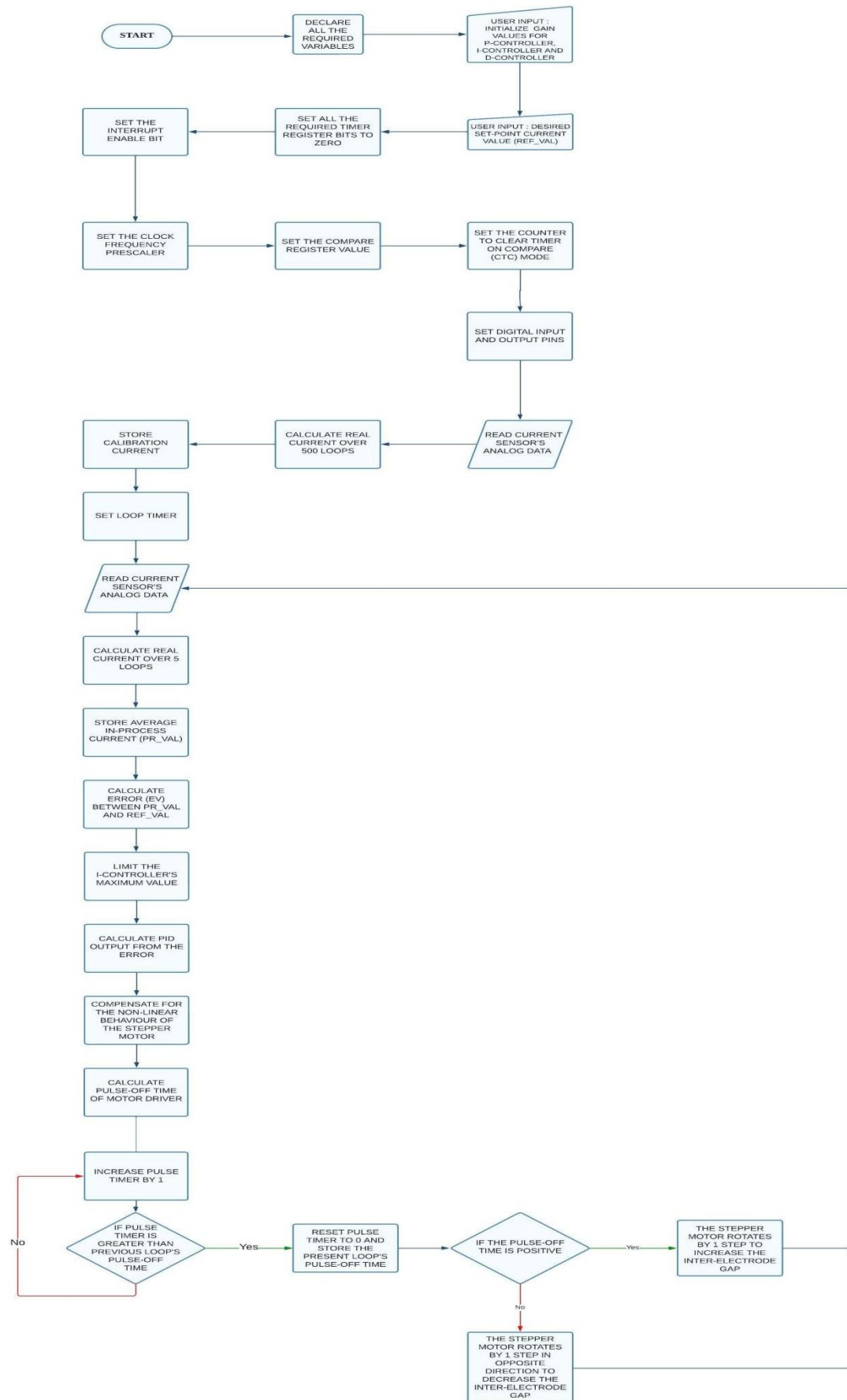


Figure 5.2: Closed loop control strategy for tool feed mechanism

Figure 5.2 shows the control strategy for the tool feed mechanism of the ECM setup and the algorithm of the code is represented through flowchart in section 5.2

5.2 FLOWCHART REPRESENTATION OF THE CODE :-



5.3 KEYWORDS AND THEIR EXPLANATIONS :-

(i) void setup() : This is a function definition statement of a predefined function named “setup”. Any new program in the Arduino IDE has two functions already defined in it. They are “setup” and “loop”. Both are of void return-type by default. Setup function is called only once when the Arduino unit powers up or is reset by button. This is a great place to initialize input and output pins, initialize variables, start using libraries, etc.

(ii) Serial.begin(9600) : Serial.begin() establishes serial communication between your Arduino board and another device. The most common use of this function is to establish communication between the Arduino and computer via a USB cable – or an Universal **Serial** Bus cable. When serial communication happens between two devices, it allows the two devices to communicate using a serial protocol. The number 9600 sets the data rate in bits per second (baud) for serial data transmission with the serial monitor.

(iii) TCCR2A : This stands for Timer Counter Control Register 2A.

(iv) TCCR2B : This stands for Timer Counter Control Register 2B.

ATmega328P has three timers, namely, TIMER 0, TIMER 1, TIMER2. TIMER 0 and TIMER 2 are 8-bit timers, hence count from 0 to 255 and again reset to 0. TIMER 1 is a 16-bit timer, hence counts from 0 to 65535 and then resets to 0. TCCR2A and TCCR2B are registers of TIMER 2. Each bit of the registers can be either of read-only or read-write mode. The timers can be made to serve different purposes according to our will by setting different combination of zeroes and ones in the registers. General uses of these timers include:

- Turn on or turn off an external device at a programmed time.
- Generate a precision output signal (period, duty cycle, frequency). For example, generate a complex digital waveform with varying pulse width to control the speed of a DC motor.
- Measure the characteristics (period, duty cycle, frequency) of an incoming digital signal.
- Count external events

(v) **TIMSK2** : This is the keyword for Interrupt Mask Register of Timer 2. All the interrupts are individually masked with the timer interrupt mask register.

(vi) **OCIE2A** : This stands for Timer 2 Output Compare Match A Interrupt Enable.

Bit	7	6	5	4	3	2	1	0	
(0x70)	–	–	–	–	–	OCIE2B	OCIE2A	TOIE2	TIMSK2
Read/Write	R	R	R	R	R	R/W	R/W	R/W	
Initial Value	0	0	0	0	0	0	0	0	

Table 5.1: TIMSK2 register map

When the OCIE2A bit is written to one and the I-bit in the status register is set (one), the Timer2 compare match A interrupt is enabled. The corresponding interrupt is executed if a compare match in Timer2 occurs.

(vii) **CS21** : This is a clock select bit of TCCR2B.

Bit	7	6	5	4	3	2	1	0	
(0xB1)	FOC2A	FOC2B	–	–	WGM22	CS22	CS21	CS20	TCCR2B
Read/Write	W	W	R	R	R	R	R/W	R/W	
Initial Value	0	0	0	0	0	0	0	0	

Table 5.2: TCCR2B register map

CS22	CS21	CS20	Description
0	0	0	No clock source (Timer/Counter stopped).
0	0	1	$clk_{T2S}/(no\ prescaling)$
0	1	0	$clk_{T2S}/8$ (from prescaler)
0	1	1	$clk_{T2S}/32$ (from prescaler)
1	0	0	$clk_{T2S}/64$ (from prescaler)
1	0	1	$clk_{T2S}/128$ (from prescaler)
1	1	0	$clk_{T2S}/256$ (from prescaler)
1	1	1	$clk_{T2S}/1024$ (from prescaler)

Table 5.3: Clock Select Bit description

The three clock select bits select the clock source to be used by the Timer. If only CS21 bit is enabled, frequency of clock, i.e., 16 MHz is prescaled by 8 to become 2MHz.

(viii) **OCR2A** : This stands for Output Compare Register 2A. The output compare register A contains an 8-bit value that is continuously compared with the counter value (TCNT2). A match can be used to generate an output compare interrupt.

(ix) **WGM21** : This is a bit in the register TCCR2A, WGM stands for waveform Generation Mode. Combined with the bit WGM22 and WGM20, these bits control the counting sequence of the counter and what type of waveform generation to be used. When only 1 is set on WGM21 bit and WGM22, WGM20 have zeroes, then the timer works on CTC mode(Clear Timer on Compare Match).

Bit	7	6	5	4	3	2	1	0	
(0xB0)	COM2A1	COM2A0	COM2B1	COM2B0	–	–	WGM21	WGM20	TCCR2A
Read/Write	R/W	R/W	R/W	R/W	R	R	R/W	R/W	
Initial Value	0	0	0	0	0	0	0	0	

Table 5.4: TCCR2A Register map

(x) **CTC mode**: CTC stands for Clear Timer on Compare Match mode. In CTC mode the counter is cleared to zero when the timer counter value (TCNT2) matches the OCR2A. The OCR2A defines the top value for the counter, hence also its resolution.

Assigning proper bits with required values enable the Interrupt Service Routine (ISR) to be called after every 20 μ s. This is the time required for the Timer counter 2 (TCNT2) to match the value 39 defined in the compare register (OCR2A) and then resets to 0 as per CTC mode.

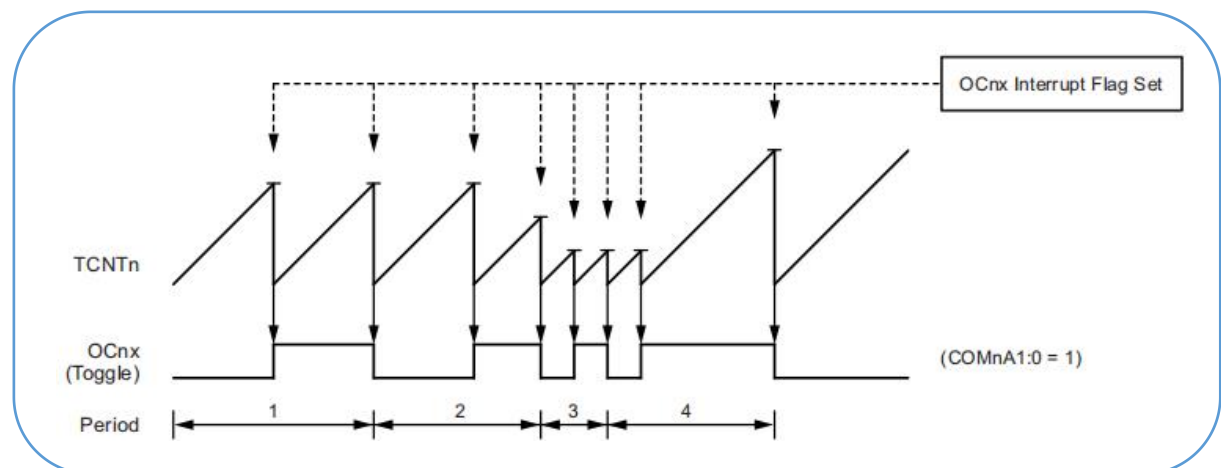


Figure 5.3: CTC Mode, Timing diagram

(xi) **pinMode(argument 1, argument 2)** : This command initializes a pin to perform in output or input mode. This is the call statement to an inbuilt function “pinMode”. It takes two arguments, argument 1 states the pin number which we want to initialize, argument 2 states the mode either input or output.

(xii) digitalWrite(argument 1, argument 2) : This command is used to write either high (on) or low (off) value to a digital output pin. Argument 1 takes the pin number and argument takes “high” or “low” as input. “digitalWrite” is an inbuilt function and has no return-type.

(xiii) digitalRead(argument 1) : This is a function call statement used to judge whether an input pin is in high or low state. Argument 1 receives the pin number whose mode is to be known and returns “HIGH” or “LOW” value thus checking whether any voltage is applied to that pin or not.

(xiv) analogRead(argument 1) : This function is used to read the voltage applied to any of the six analog input pins. Argument 1 takes the pin number whose voltage is to be known. It returns a value between 0 and 1023 which represents voltage between 0 and 5 V. This is done by linear interpolation method.

(xv) PORTD : This command is used to write binary codes 0 and 1 to digital pins 0 to 7. For example, if we state `PORTD = 0B00001000`, we are instructing the processor to set digital pin 3 as “high” or “on”.

5.4 VARIABLE DESCRIPTION :-

This section will give the details about all the variables used in the program.

<u>Variable name</u>	<u>Variable datatype</u>	<u>Variable description</u>
pid_p_gain	float	Used to store the P-controller gain value
pid_i_gain	float	Used to store the I-controller gain value
pid_d_gain	float	Used to store the D-controller gain value
current	float	Used to store the current value in amperes
cur	float	Used to store the reading of analog pin A1
sum	float	Used to store sum of the current readings
avc	float	Used to store average current reading
current_calib	float	Used to store calibration current reading
pr_val	float	Used to store in-process current reading
ref_val	float	Used to store set-point current reading
ev	float	Used for storing error between pr_val & ref_val
last_ev	float	Used to store error of the last loop
pid_i_mem	float	Used to store output of the I-controller
loop_timer	unsigned long	Used to set loop time of 8 ms
pid_output	float	Used to store output of P-I-D controller
pid_out	float	Used to store linearized value of pid_out
x	int	Loop variable
motor	int	Used for storing pulse time of motor driver
throttle_motor	int	Store the value of motor variable for interrupt
throttle_counter	int	Counter variable for comparing with pulse time
motor_memory	int	Store the next pulse time for motor driver

Table 5.5: Variable description

Experiments of electrochemical drilling have been done using the in-house developed mini ECM setup to examine the machining accuracy and precision of the through holes made in the workpiece. A round hollow Brass bar of average outer diameter 2.1 mm has been used as the tool (cathode) and Aluminium sheet of average thickness 3.2 mm as workpiece (anode).

6.1 EFFECT OF INSULATION :-

To avoid formation of radial overcuts, the tip of the tool had been insulated by manually depositing a thin film of strong metal adhesive (gray in colour) around the tip as shown in figure 6.1. Diameter of the tool with insulation was 2.18 mm. Proper care had been taken during this method, so that hollow cross-sectional area remained exposed as displayed in figure 6.2. Initially, commercial instant adhesives meant for PVC bonding were used. But, these kinds of insulations got wore away easily particularly from around the tip, due to the flow of high pressurized electrolyte mixed with sludge in the machining zone. This resulted in greater metallic surface area exposure for conduction and eventually the machining current increased. The control strategy being based on closed-loop algorithm, the controller learnt that inter-electrode gap current was high and the tool got automatically retrieved from the workpiece. Through-hole drilling process became unsuccessful. The results were formation of both narrow and wide craters on the workpiece. Size of the craters depended on controller's gain values. Figure 6.3 shows the failures of through-hole drilling process collectively.



Figure 6.1: Hollow brass tool with insulated tip



Figure 6.2: Exposed hollow cross-section

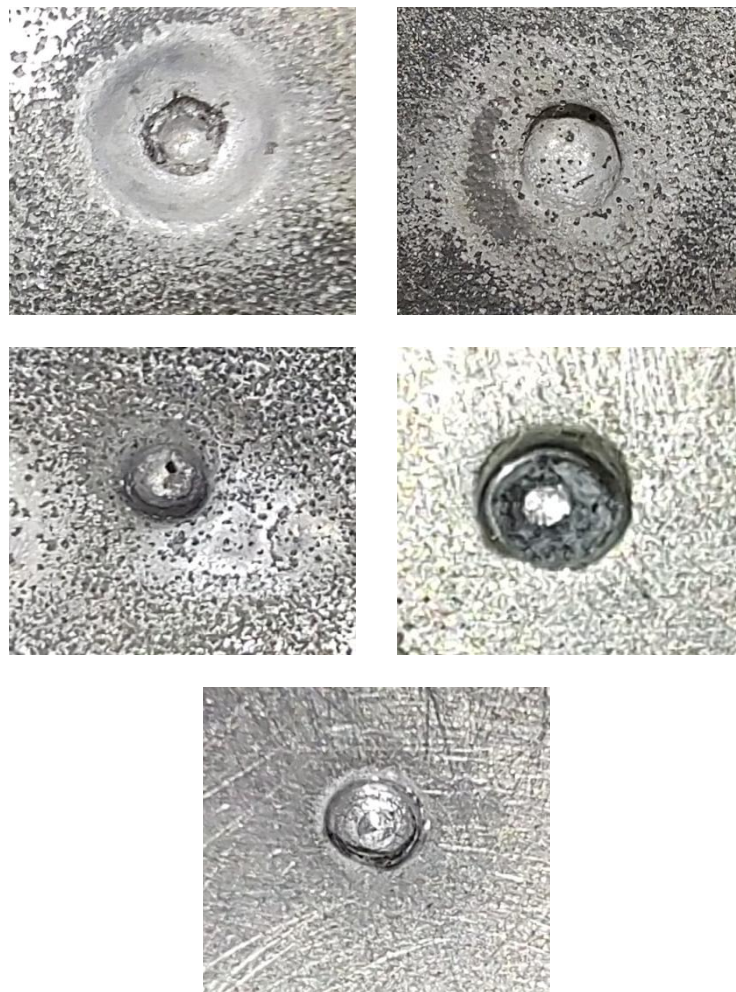


Figure 6.3: Failures of through-hole drilling process

6.2 EFFECT OF P - I - D CONTROLLER GAIN SETTINGS :-

6.2.1 EFFECT OF ONLY PROPORTIONAL ACTION :

In this case, the control signal only consists of the P-term, which is proportional to the error between the set-point reference current value and the in-process inter-electrode gap current value. The controller acts on the present value of the error and the output never reaches the steady state error. It results in a to-and-fro unsteady motion of the tool along z-axis. Through hole drilling takes place but the machining time is very long and radial overcut is noticed. Also, there remains risks of short-circuit in the inter-electrode gap, leading to tool wear, low surface finish and insulation wear-out. Pictures of holes drilled with proportional action are given below.

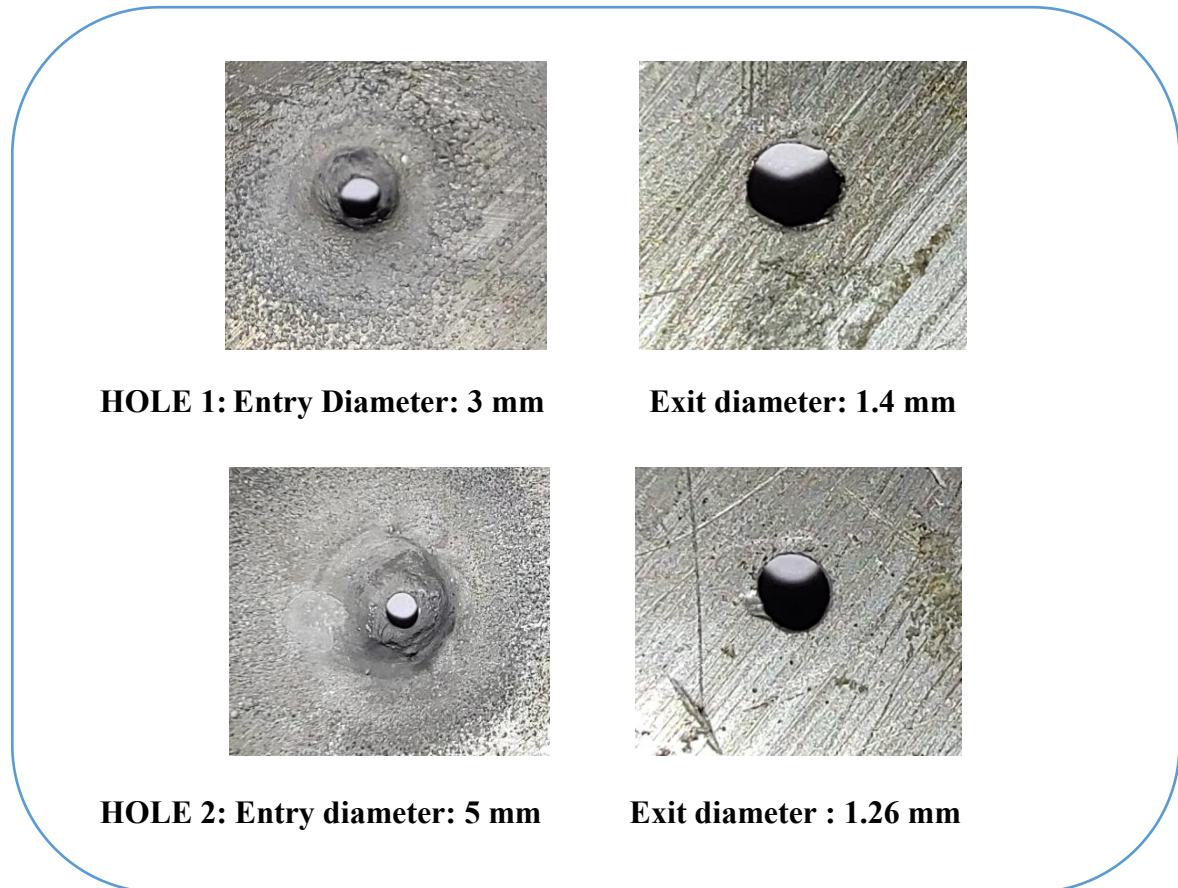


Figure 6.4: Holes drilled using P-action

Hole 1 has taper angle of 14.03 degrees while hole 2 has taper angle of 30.3 degrees. This is because hole 2 is drilled with low set-point current, so the machining took place for longer time.

6.2.2 EFFECT OF PROPORTIONAL AND INTEGRAL ACTION :

The scenario in this case is a bit different from the previous case. The controller keeps track of both the present and past errors. So, the amplitude of the to and fro movement increases in comparison to that of proportional action. The integral windup value plays an important role during machining. Larger its value, greater will be the chances of short-circuit between tool and workpiece.



Figure 6.5: Hole 3 drilled using P - I action

6.2.3 EFFECT OF PROPORTIONAL, INTEGRAL AND DERIVATIVE ACTION :

In this case, the proportional part acts on the present value of the error, the integral part represents an average of past errors and the derivative can be interpreted as a prediction of future errors based on linear extrapolation. The control action is steadier in comparison to the previous cases. The machining time reduces impressively. The holes are almost precise having very little difference between entry and exit diameters. Also, no short-circuits occur between tool and workpiece during machining. Images of holes drilled with this control strategy are shown in figure 6.6.

6.3 EFFECT OF USING LOW SET-POINT CURRENT :

The material removal rate is slower. Since the tool feed rate becomes very slow, electrolytic dissolution takes place through a long time. Larger diameter holes are observed in this case, with very negligible glimpses of short-circuits. Some examples are shown in figure 6.8.



HOLE 4: Entry diameter: 2.01mm



Exit diameter: 1.85 mm



HOLE 5: Entry diameter: 2.75 mm



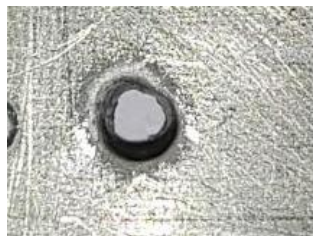
Exit diameter: 2.1 mm



HOLE 6: Entry diameter: 2.38 mm



Exit diameter: 2.05 mm



HOLE 7: Entry diameter: 2.32 mm



Exit diameter: 1.81 mm



HOLE 8: Entry diameter: 2.5 mm



Exit diameter: 1.93 mm

Figure 6.6: Holes drilled with P - I -D action

Hole 4 has taper angle of 1.43 degrees.

Hole 5 has taper angle of 5.8 degrees.

Hole 6 has taper angle of 3.02 degrees.

Hole 7 has taper angle of 4.55 degrees.

Hole 8 has taper angle of 5.1 degrees.

Clearly, it is evident that the taper angle is much less for the holes drilled with P-I-D control action than of those drilled with proportional action only.

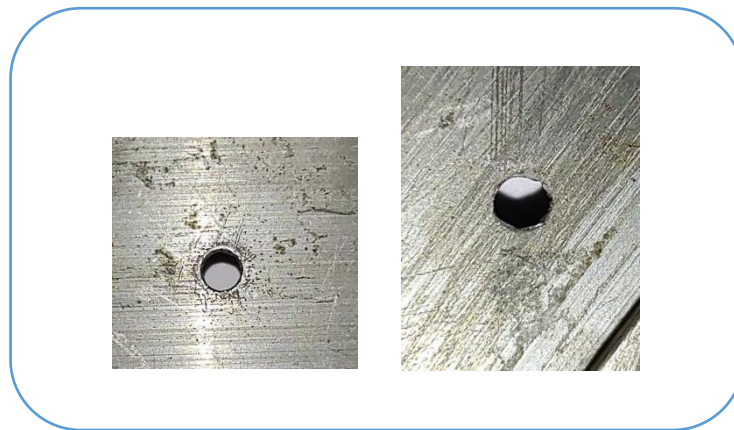


Figure 6.7: Circularity of holes at exit ends



Figure 6.8: Holes drilled with low set-point current

SUMMARY AND GENERAL CONCLUSIONS

A mini desktop ECM setup with feedback controlled tool feed mechanism has been developed. In the present research study, a mini desktop ECM setup with feedback controlled tool feed mechanism has been developed. Extruded aluminum profiles were used in the machine frame and for X, Y and Z axis movement 8 mm guide rods and lead screws were used. Due to the known capability of precise movement and generating high torque at low speed, stepper motors were used for all three axes. NEMA 17 stepper motors with torque of 2.5 kg-cm were used and connected with the motor driver DRV8825. In order to develop the closed-loop feedback control system the current sensor WCS1700 was used. Plain DC power supply systems with rated voltage and current combinations of 60V 6.67A, 24V 10A and 12V 10A respectively were incorporated. The developed electrolyte supply system was equipped with two different types of pumps in order to deliver different kinds of flow rates depending on specific machining requirements. Finally, the microcontroller was programmed using AVR C to achieve a feedback control system. Based on the present research studies the following observations can be made :

1. The framework developed with the extruded aluminium profile was quite suitable for this application and no trace of corrosion was observed. All other metallic components (e.g. lead screw guide rod etc.) in the setup were heavily coated with grease to prevent corrosion.
2. It is observed that the motor driver DRV8825 was delivering the desired result with even higher micro-stepping modes. The stepper motor driver was programmed to be used in 1/32 microstepping mode which enables very precise and accurate tool movement. The DRV8825 along with the NEMA17 stepper motor was absolutely a good combination and was giving very good performance.
3. Initially current sensor ACS712 was used for developing the feedback control system. But due to performance issues it was replaced with the current sensor WCS1700. It was observed that WCS1700 was giving quite satisfactory performance and capable of measuring current quite accurately and readings were very precise.

4. The developed electrolyte circulation system is compact, easy to assemble and made of corrosion resistant components. The supply can be done in two modes, viz. low pressure and high pressure modes using two different pumps. The variation in electrolyte concentration is negligible. Based upon the limited period of observation it can be stated that the two pumps namely the diaphragm pump (for high pressure applications) and the submersible centrifugal pump (for low pressure applications) are cheap and quite suitable solutions for this setup.
5. Hollow Brass tool is used for supplying the electrolyte directly to the machining zone. The tool is insulated at the outer surface with metal adhesive paste. This insulation coating plays an important role to avoid machining due to stray current. Else, precise deep through holes cannot be drilled.
6. The tool holder was designed and fabricated in such a way that tool replacement can be easily done without changing the alignment. A 3D-printed bench vise has been developed. The vise can hold the workpiece quite sturdily against the force of high pressure electrolyte thereby allowing no undesirable movement of the same during machining.
7. Switched Mode Power supplies are used for supplying DC power to the tool, workpiece and other electrical components in the setup. A separate SMPS was used for powering the electrode and workpiece only. The power supply system was also designed to protect from overcurrent, and short circuit conditions. Facility was there to regulate the voltage as per requirements.
8. The microcontroller ATmega328P is programmed for advanced PID motion control mechanism of the tool. The program is user-friendly, and can be easily modified to use for various electrochemical processes that can take place in the same mechanical setup.

However, there lies a scope for future upgradation of the setup. Drilling positions can be moved along X and Y axes simultaneously thereby creating a drilling pattern on the XY plane of the workpiece. Also pulsed DC power supply module can be developed instead of using a continuous DC power supply module. This will improve the machining accuracy and

surface roughness. Thirdly, a jet ECM setup can also be fabricated from this existing setup. Indeed, there can be numerous such developments from one single setup.

Hence, it can be concluded that the developed ECM setup is very cheap in comparison to other commercial machines available in the market. Yet, this setup offers feedback control strategy and non-corrosive components promise good endurance of the setup with very little maintenance. These advantages enable it to be used in small-scale industries, research institutions and has lot of other potential applications in modern manufacturing industries. Truly, such developments are cornerstones in manufacturing science and technology.

- [1] Dayanand S. Bilgi, V. K. Jain, R. Shekhar and Anjali V. Kulkarni, “Hole quality and inter-electrode gap dynamics during pulse current electrochemical deep hole drilling”, *International Journal of Advanced Manufacturing Technology*, 2007, 34: 79-95.
- [2] B. Bhattacharyya, M. Malapati and J. Munda, “Experimental study on electrochemical micromachining”, *Journal of Materials Processing Technology*, 2005, 169: 485-492.
- [3] Alexandre Spieser and Atanas Ivanov, “Design of an Electrochemical Micromachining Machine”, *International Journal of Advanced Manufacturing Technology*, 2015, 78: 737-752.
- [4] A.W. Labib, V.J. Keasberry, J. Atkinson and H.W. Frost, “Towards next generation electrochemical machining controllers: A fuzzy logic control approach to ECM”, *Expert Systems With Applications*, 2011, 38: 7486-7493.
- [5] Chaojiang Li, Bowei Zhang, Yong Li, Hao Tong, Songlin Ding, Zhiqiang Wang and Lei Zhao, “Self-adjusting EDM/ECM high speed drilling of film cooling holes”, *Journal of Materials Processing Tech.*, 2018, 262: 95-103.
- [6] Wei Chen and Fuzhu Han, “Short-circuit avoidance in electrochemical machining based on polarization voltage during pulse off time”, *International Journal of Advanced Manufacturing Technology*, 2019, 102: 2531-2539.
- [7] S. Saranya and A. Ravi Sankar, “A Microcontroller-based Electrochemical Discharge Machining (ECDM) Equipment for Micro-drilling of Quartz Substrates”, *IEEE International Symposium on Smart Electronic Systems (iSES) (Formerly iNiS)*, 14-16 December 2020, Chennai, India.
- [8] J. Kozak, M. Chuchro, A. Ruszaj and K. Karbowski, “The computer aided simulation of electrochemical process with universal spherical electrodes when machining sculptured surfaces”, *Journal of Material Processing Technology*, 2000, 107: 283– 287.
- [9] Wenjian Cao , Dengyong Wang and Di Zhu, “Modeling and experimental validation of inter-electrode gap in counter-rotating electrochemical machining”, *International Journal of Mechanical Sciences*, 2020, 187: Article no. 105920.
- [10] N.K. Jain and V.K. Jain, “Optimization of Electro-Chemical Machining Process Parameters Using Genetic Algorithms”, *Machining Science and Technology*, April 2007, Volume 11, Number 2: 235-258.

- [11] Y. Ye, H. Lianhuan, H. Di, S. Jian-Jia, T. Zhong-Qun, T. Zhao-Wu and Z. Dongping, “Electrochemical Micromachining under Mechanical Motion Model”, *Electrochimica Acta*, 2015, 187: 3-7.
- [12] Jinxing LUO, Xiaolong FANG, Tao YANG and Di ZHU, “Electrochemical drilling of small holes by regulating in real-time the electrolyte flowrate in multiple channels”, *Chinese Journal of Aeronautics*, 2022, 35(5): 470-483.
- [13] W. Vanderauweraa, M. Vanloffelta, R. Perezb and B. Lauwersa, “Investigation on the performance of macro electrochemical milling”, *Procedia CIRP*, 2013, 6: 356-361.
- [14] S.Aravind and Somashekhar S. Hiremath, “Design and Development of IEG Control and Characterization of Micro-holes Generated Using In-house Developed μ -ECM Setup”, *Arabian Journal for Science and Engineering*, 2022, 47: 8877–8898.
- [15] Lizhong Xu, JipengWang and Chuanjun Zhao, “Electrochemical micro-machining based on double feedback circuits”, *Scientific Reports*, Issue 13, 2023, Article no. 319.